



DEVELOPMENT OF POLY(LACTIC ACID) TERNARY BLENDS PROPERTIES FOR
PLASTIC PACKAGING APPLICATIONS BY THERMOFORMING TECHNIQUE



A Thesis Submitted in Partial Fulfillment of the Requirements
for Master of Engineering (CHEMICAL ENGINEERING)

Department of CHEMICAL ENGINEERING

Graduate School, Silpakorn University

Academic Year 2022

Copyright of Silpakorn University

การพัฒนาสมบัติของพอลิแลคติกแอซิดผสมสามองค์ประกอบเพื่อประยุกต์ใช้เป็นบรรจุ
ภัณฑ์พลาสติกด้วยเทคนิคเทอร์โมฟอร์มมิ่ง



วิทยานิพนธ์นี้เป็นส่วนหนึ่งของการศึกษาตามหลักสูตรวิศวกรรมศาสตรมหาบัณฑิต

สาขาวิชาวิศวกรรมเคมี แผน ก แบบ ก 2 ระดับปริญญามหาบัณฑิต

ภาควิชาวิศวกรรมเคมี

บัณฑิตวิทยาลัย มหาวิทยาลัยศิลปากร

ปีการศึกษา 2565

ลิขสิทธิ์ของมหาวิทยาลัยศิลปากร

DEVELOPMENT OF POLY(LACTIC ACID) TERNARY BLENDS PROPERTIES
FOR PLASTIC PACKAGING APPLICATIONS BY THERMOFORMING
TECHNIQUE



A Thesis Submitted in Partial Fulfillment of the Requirements
for Master of Engineering (CHEMICAL ENGINEERING)
Department of CHEMICAL ENGINEERING
Graduate School, Silpakorn University
Academic Year 2022
Copyright of Silpakorn University

Title Development of poly(lactic acid) ternary blends properties for plastic packaging applications by thermoforming technique

By MISS Laoongpun WONGWAD

Field of Study (CHEMICAL ENGINEERING)

Advisor Associate Professor Sirirat Wacharawichanant, D.Eng.

Graduate School Silpakorn University in Partial Fulfillment of the Requirements for the Master of Engineering

.....Dean of the Graduate School
(Assistant Professor Sathit Niratisai, Ph.D.) (Acting)

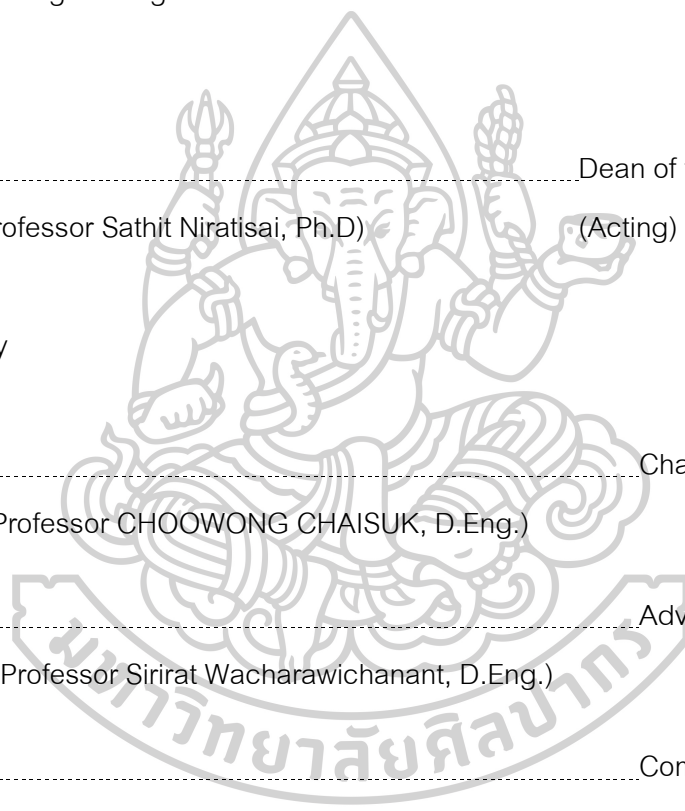
Approved by

.....Chair person
(Assistant Professor CHOOWONG CHAISUK, D.Eng.)

.....Advisor
(Associate Professor Sirirat Wacharawichanant, D.Eng.)

.....Committee
(Associate Professor Prakorn Ramakul, D.Eng.)

.....External Examiner
(Professor Anongnat Somwangthanaroj, Ph.D.)



59404209 : Major (CHEMICAL ENGINEERING)

Keyword : poly(lactic acid) poly(butylene succinate) ethylene-propylene-diene rubber polymer blends

MISS LAOONGPUN WONGWAD : DEVELOPMENT OF POLY(LACTIC ACID) TERNARY BLENDS PROPERTIES FOR PLASTIC PACKAGING APPLICATIONS BY THERMOFORMING TECHNIQUE THESIS ADVISOR : ASSOCIATE PROFESSOR SIRIRAT WACHARAWICHANANT, D.Eng.

This research was aimed to study the poly(lactic acid) (PLA) blends between poly(butylene succinate) (PBS) and ethylene-propylene-diene rubber (EPDM) for thermoforming. The objectives of this type of ternary blends were to study some properties such as morphology, mechanical properties and thermal properties. which is divided into two component blends and three components. This research was divided into 2 parts. The first part studied PLA and PBS blends ratio at PLA/PBS (90/10), PLA/PBS (80/20) and PLA/PBS (70/30). After that finding the suitable ratio, the second part studied PLA/PBS (80/20) and EPDM ternary blends at ratio PLA/PBS/EPDM (80/15/5), PLA/PBS/EPDM (80/10/10) and PLA/PBS/EPDM (80/5/15). The sample can be molded by thermoforming. The polymer blends were prepared via internal mixer and sample films was prepared by compression molding. The results found that the morphological analysis observed the phase separation of PLA/PBS, PLA/EPDM and PLA/PBS/EPDM ternary blends and showed the minor phase dispersed in PLA matrix phase. The domain size of EPDM phase in PLA/PBS/EPDM ternary blends increased with the increase of EPDM contents. The results of tensile properties showed that Young's modulus of PLA/PBS (80/20) blends was higher than that of PLA/EPDM (80/20) and PLA/PBS/EPDM ternary blends. While the strain at break of PLA/EPDM (80/20) blends was higher than that of PLA/PBS (80/20) blends and the strain at break of ternary blends increased with increasing EPDM content, this indicated the presence of EPDM enhanced the strain at break of PLA. Additionally, the ternary blends of PLA/PBS/EPDM (80/5/15) exhibited higher impact strength than pure PLA.



ACKNOWLEDGEMENTS

The author wished to express her gratitude and appreciation to an advisor, Associate Professor Sirirat Wacharawichanant for their support, stimulating, useful discussions throughout this research and devotion to revise this thesis otherwise it cannot be completed in a short time.

In addition, the author would like to gratefully acknowledge Assistant Professor Choowong Chaisuk, as the chairman of the committee, Associate Professor Prakorn Ramakul, Associate Professor Dr. Anongnate Somwangthanoj and Dr. Sunthon Piticharoenphun as the members of thesis committee for their kind evaluation of work and valuable suggestions that could be beneficially used to improve working behavior.

In particular, special thanks for the kind suggestions and useful help to members of Polymer Innovation Laboratory and members of the research zone for their assistance. The author would like to thank the center of excellence on Catalysis and Catalytic reaction

Engineering, Department of Chemical Engineering, Faculty of Engineering, Chulalongkorn University for differential scanning calorimeter (DSC), thermogravimetric analysis (TGA), dynamic mechanical analyzer (DMA), ultraviolet-visible spectroscopy (UV-Vis) and X-Ray Diffractometer (XRD).

Most importantly, the author would like to express the highest gratitude to my family and my best friend, who always supported pay attention to though these years for their encouragement, love, care, and other their will.

MISS Laoongpun WONGWAD

TABLE OF CONTENTS

	Page
ABSTRACT	D
ACKNOWLEDGEMENTS.....	F
TABLE OF CONTENTS.....	G
LIST OF TABLES.....	K
LIST OF FIGURES	L
CHAPTER 1 INTRODUCTION.....	1
1.1 The Statement and Significance of problems	1
1.2 Objectives of the research work.....	3
1.3 Scope of the research work.....	3
CHAPTER 2 THEORY.....	4
2.1 Polylactic Acid (PLA)	4
2.2 Polybutylene Succinate (PBS)	6
2.3 Ethylene-Propylene Diene Monomer (EPDM).....	7
2.4 Polymers Blends	8
2.5 Thermoforming Process.....	10
2.6 Mechanical Analysis	10
2.6.1 Universal tensile testing	10
2.6.2 Impact testing.....	11
2.7 Scanning Electron Microscopy (SEM).....	12
2.8 Thermal Analysis.....	16
2.8.1 Differential Scanning Calorimetry (DSC).....	16

2.8.2 Thermogravimetric Analysis (TGA)	18
2.9 Chemical Structure and Interaction	18
2.9.1 Fourier-Transform Infrared Spectroscopy (FTIR).....	18
2.10 Crystal Structure	19
2.10.1 X-Ray Diffraction (XRD)	19
2.11 Ultraviolet-Visible Spectroscopy (UV-vis).....	20
CHAPTER 3 LITERATURE REVIEWS	21
CHAPTER 4 METHOD OF RESEARCH	26
4.1 Materials	26
4.1.1. Poly(Lactic Acid), (PLA)	26
4.1.2. Poly(Butylene Succinate), (PBS)	26
4.1.3. Ethylene-Propylene Diene Monomer (EPDM).....	27
4.2 Preparation of Materials	28
4.2.1 Preparation of PLA/PBS blends	28
4.2.2 Preparation of PLA/PBS/EPDM ternary blends.....	28
4.3 Sample Preparation	30
4.3.1 Dog bone or Dumbbells shape	30
4.3.2 Bar shape	30
4.3.3 Film or sheet shape	30
4.4 Sample characterization	31
4.4.1 Tensile test.....	31
4.4.2 Impact test.....	32
4.4.3 SEM observation	33

4.4.4 Differential scanning calorimetry, (DSC).....	34
4.4.5 Thermogravimetric analysis, (TGA).....	35
4.4.6 Dynamic mechanical analyzer (pyris diamond DMA)	36
4.4.7 X-Ray diffractometer analysis (XRD).....	37
4.4.8 Fourier-Transform Infrared Spectroscopy (FTIR).....	38
4.4.9 Ultraviolet visible spectroscopy (UV-vis)	38
4.4.10 Thermoforming test	38
CHAPTER 5 RESULTS AND DISCUSSION.....	40
5.1 Morphology Properties.....	40
5.1.1 PLA/PBS blends	40
5.1.2 PLA/PBS/EPDM ternary blends.....	41
5.2 Mechanical properties	46
5.2.1 Impact properties.....	46
5.2.2 Tensile properties.....	47
5.2.2.1 PLA/PBS blends.....	47
5.2.2.2 PLA/PBS/EPDM ternary blends	50
5.3 Thermal properties	55
5.3.1 DSC analysis	55
5.3.1.1 The Melting point temperature (T_m)	55
5.3.1.2 Percentage crystallinity.	58
5.3.2 TGA analysis.....	59
5.4 Thermomechanical Properties	61
5.4.1 PLA/PBS blends	61

5.4.2 PLA/PBS/EPDM ternary blends.....	61
5.5. XRD analysis	64
5.6. FTIR analysis	67
5.7. UV- vis analysis.....	69
5.8. Packaging from thermoforming	72
5.8.1 PLA/PBS blends	72
5.8.2 PLA/PBS/EPDM ternary blends.....	72
CHAPTER 6 CONCLUSION.....	77
6.1 Morphological Properties.....	77
6.2 Mechanical Properties	77
6.3 Thermal Properties.....	77
6.4 Thermomechanical Properties.....	77
6.5 FT-IR Analysis	78
6.6 UV-vis analysis.....	78
6.7 Packaging from Thermoforming	78
REFERENCES.....	79
VITA	85

LIST OF TABLES

	Page
Table 1 Comparison of exemplary physical properties of PBS compared to other (bio based) polymers.....	7
Table 2 Composition of the prepared binary and ternary blends.	29
Table 3 Young's modulus and tensile strength of PLA pure, PBS pure, PLA/PBS blends, PLA/PBS/EPDM ternary blends, and PLA/EPDM blends.....	54
Table 4 Stress at break and strain at break of PLA pure, PBS pure, PLA/PBS blends, PLA/PBS/EPDM ternary blends, and PLA/EPDM blends.....	54
Table 5 Melting point temperature (T_m) and percentage crystallinity ($\%X_c$) of PLA pure, PBS pure, PLA/PBS, PLA/EPDM blends and PLA/PBS/EPDM ternary blends.....	56
Table 6 Decomposition temperature of PLA, PLA/PBS and PLA/PBS/EPDM.	60
Table 7 Normalized crystallinity of blends and ternary blends.	66



LIST OF FIGURES

	Page
Figure 1 Different routes to produce PLA. [4].....	5
Figure 2 Schematic representation of PBS synthesis from SA and BDO. (a) esterification, (b) transesterification [10].	6
Figure 3 Typically, dicyclopentadiene, ethylidene norbornene, or 1,4 hexadiene is the diene. These terpolymers may be vulcanized using conventional methods.	7
Figure 4 Vacuum forming procedure. a. Heating the flat sheet. b. The space between the softened sheet and the mold is evacuated, forcing the sheet to conform to the shape of the mold. [14].	10
Figure 5 The electron column displays all of the signal-related components from their emission to their capture. In the cabinet, signals are processed to facilitate display [17].	13
Figure 6 Schematic illustrations the components of scanning electron microscopes [18].	14
Figure 7 Illustrates typical polymer DSC thermograms [22].....	17
Figure 8 Morphology of NR droplet size in PLA/NR blends at different NR concentrations (a) 5 wt%, (b) 10 wt% and (c) 20 wt%. [29].....	22
Figure 9 Shows tensile strength of the PP/EPDM/PLA blends with. PLA content and hydrolysis time. [30]	23
Figure 10 Reactions that are initiated by DCP, producing macromolecular free radicals, include NR and PLA (RO is for cumyloxy radical).[31]	24
Figure 11 SEM images of freeze-fracture surface of a PLA, b 0.5 wt% DCP/PLA, c PLA/NR and d 2 wt% DCP/PLA/NR. [31]	24
Figure 12 PLA commercial name Ingeo Biopolymer 2003D.....	26

Figure 13 Poly(butylene succinate), (PBS).....	27
Figure 14 Ethylene propylene diene monomer rubber (EPDM rubber).	27
Figure 15 Internal mixer.....	29
Figure 16 Compression molding machine.....	31
Figure 17 Universal tensile testing machine.....	32
Figure 18 Impact testing machine.	33
Figure 19 MIRA3 FEG-SEM (A Flexible Scanning Electron Microscope).....	34
Figure 20 Thermogravimetric analysis, (TGA)	35
Figure 21 X-Ray Diffractometer (Bruker AXS Model D8 Discover).....	38
Figure 22 Thermoforming machine	39
Figure 23 SEM micrographs of the tensile fracture surface of PLA, PBS and PLA/PBS blends at various PBS contents.	44
Figure 24 micrographs of the tensile fracture surface of PLA/PBS/EPDM ternary blends.....	45
Figure 25 Impact Strength of pure PLA, pure PBS, PLA/PBS blends and PLA/PBS/EPDM ternary blends at different compositions.	46
Figure 26 Young's modulus of pure PLA, pure PBS and PLA/PBS blends at different compositions.	48
Figure 27 Tensile strength of pure PLA, pure PBS and PLA/PBS blends at different compositions.	48
Figure 28 Stress at break of pure PLA, pure PBS and PLA/PBS blends at different compositions.	49
Figure 29 Percent strain at break of pure PLA, pure PBS and PLA/PBS blends at different compositions.	49
Figure 30 Young's modulus of PLA/PBS/EPDM ternary blends.	52

Figure 31 Tensile strength of PLA/PBS/EPDM ternary blends.	52
Figure 32 Stress at break of PLA/PBS/EPDM ternary blends.	53
Figure 33 Percent strain at break of PLA/PBS/EPDM ternary blends.....	53
Figure 34 DSC graph of PLA pure, PBS pure, and PLA/PBS blends.....	57
Figure 35 DSC graph of PLA pure, PLA/PBS blends, PLA/EPDM blends, and PLA/PBS/EPDM ternary blends.....	57
Figure 36 TGA thermograms of PLA PLA/PBS and PLA/PBS/EPDM blends.	60
Figure 37 Storage modulus of pure PLA and PLA/PBS blends with PBS contents.	62
Figure 38 Storage modulus of pure PLA and PLA/PBS/EPDM ternary blends with EPDM contents.....	63
Figure 39 The XRD patterns of pure PLA, pure PBS and pure EPDM.	65
Figure 40 The XRD patterns of pure PLA, and PLA/PBS blends with various weight ratios.....	65
Figure 41 The XRD patterns of pure PLA, and PLA/PBS/EPDM ternary blends with various weight ratios.....	66
Figure 42 FTIR spectra of PLA pure, PLA/PBS (80/20), PLA/EPDM (80/20) and PLA/PBS/EPDM ternary blends with various ratio.....	68
Figure 43 UV-vis of PLA, PBS and EPDM.....	70
Figure 44 UV-vis of PLA and PLA/PBS blend various contents.	70
Figure 45 UV-vis of PLA and PLA/PBS/EPDM ternary blend various contents.	71
Figure 46 Neat PLA packaging from thermoforming.....	73
Figure 47 PLA/PBS (90/10) packaging from thermoforming.....	73
Figure 48 PLA/PBS (80/20) packaging from thermoforming.....	74
Figure 49 PLA/PBS (70/30) packaging from thermoforming.....	74

Figure 50 PLA/PBS/EPDM (80/15/5) packaging from thermoforming 75

Figure 51 PLA/PBS/EPDM (80/10/10) packaging from thermoforming 75

Figure 52 PLA/PBS/EPDM (80/5/15) packaging from thermoforming 76



CHAPTER 1

INTRODUCTION

1.1 The Statement and Significance of problems

Presently, the expansion in the demand for plastic is being driven by utilization value because plastic is the most advantageous material option for a wide range of applications due to the fact that it is very inexpensive. Nevertheless, the repercussions of unchecked waste management of plastics after their first usage, which contributes to the contamination of land, rivers, and oceans as well as the effects on biological food chains, are significant. While the growing problem of marine pollution caused by plastic waste has become an issue that is of great interest to people all around the world. Many countries have continuously tried to solve the problem of plastic waste by focusing on reducing the amount of waste and promoting the use of alternative materials such as "bioplastic" which is becoming a new trend in the world [1].

Bioplastic means biodegradable plastic that contains at least one important component as a biopolymer. And raw materials used in production, wholly or in part, are raw materials that can be produced or grown as a replacement (Renewable raw materials). Therefore, biopolymers produced from agricultural raw materials are receiving great interest. Since they degrade more readily than commodity fossil-fuel derived plastics, and most importantly, it is also environmentally friendly as well. Biopolymer emits substantially fewer greenhouse gases than polymers derived from petroleum. Which biopolymers are derived from agricultural raw resources, including polylactic acid (PLA), polybutylene succinate (PBS), polybutylene adipate terephthalate (PBAT), natural rubber and nylon 11, etc.

PLA can be alternatively used for plastic production instead of raw materials deriving petroleum. PLA is a biopolymer produced from agricultural starch-containing raw materials such as sugarcane, corn, and cassava. The production process begins

with mashing or grinding cassava into fine flour. Then, flour is digested into sugar and fermented with lactic acid-producing microorganisms. After that, lactic acid is polymerized into Lactide. Then, distillation in a vacuum system is employed to change the structure to polylactide or PLA. PLA is widely used in packaging, medicine, and agriculture processes [2]. PLA is an option for plastic that is better for the environment due to the fact that it is biodegradable and the manufacturing process that it undergoes is more ecologically friendly. PLA has the potential to break down into its constituent parts in under a month under the appropriate conditions [3, 4], in contrast to the conventional polymers, which require a significant amount of time to deteriorate. According to the findings of an independent study conducted by Nature Works [5]. The production of PLA requires 65% less energy than the production of conventional plastics. In addition to this, it results in the production of 68% fewer greenhouse gases. In addition, when bioplastics are burned, they do not release hazardous gases like their oil-based counterparts do [6]. And can also transfer heat and moisture well heat resistant from 60-120 °C. However, there is some disadvantage which is poor toughness [7].

PBS is a biodegradable plastic of polyester type another type is produced from 2 main monomers, succinic acid. Succinic acid is produced from plants while 1,4-butanediol is produced from petroleum. PBS is similar to polyethylene or PE which is opaque and can be easily molded into various types of processes, especially injection molding, film blowing, and thermoforming. PBS can withstand temperatures from 80-95 °C. It provides good flexibility and can also be mixed with PLA because of the improvement of properties to suit many types of products as well. Therefore, the blending of PLA and PBS was studied in this work.

From the reasons mentioned above, therefore, the researcher has the aim of this research is the development and characterizations of biodegradable PLA blend and forming with thermoforming for packaging applications

1.2 Objectives of the research work

To improve the mechanical and thermal properties of PLA/PBS/EPDM ternary blends for plastic packaging by thermoforming.

1.3 Scope of the research work

1.3.1 PLA is used as the polymer matrix.

1.3.2 Polybutylene succinate (PBS) and ethylene-propylene diene monomer (EPDM) are used as the property modifier of PLA.

-The contents of PBS are used at 10 - 30 wt%.

-The contents of EPDM are used at 5 - 20 wt%.

1.3.3 Polymer blends are prepared by melt blending in an internal mixer and molded by a compression molding.

1.3.4 Mechanical properties of polymer blends are investigated by tensile testing and impact testing.

1.3.5 Thermal properties of polymer blends are investigated by DSC, TGA and DMA.

1.3.6 Morphological properties of polymer blends are observed by SEM.

1.3.7 The polymer blends are formed to packaging by thermoforming machine which was built in our laboratory.

CHAPTER 2

THEORY

2.1 Polylactic Acid (PLA)

PLA is a linear aliphatic thermoplastic polyester that is derived from lactic acid. Lactic acid is obtained from the fermentation of plant sources that are both renewable and biodegradable, such as corn or rice starches and sugar feedstocks. PLA is a thermoplastic material with a linear molecular structure. The chemical transformation of corn or other sources of carbohydrates into dextrose is one method that can be used to create it. The fermentation of dextrose results in the production of lactic acid, which is then followed by the polycondensation of lactic acid monomers, also known as lactide. However, the ring opening polymerization of lactide monomer that is generated from lactic acid is the most prevalent method that is used to make PLA [8]. The many ways that PLA can be manufactured are outlined in Figure 1. According to some reports, the production of PLA resin pellets requires anywhere from 25 to 55% less fossil energy than the production of petroleum-based polymers.



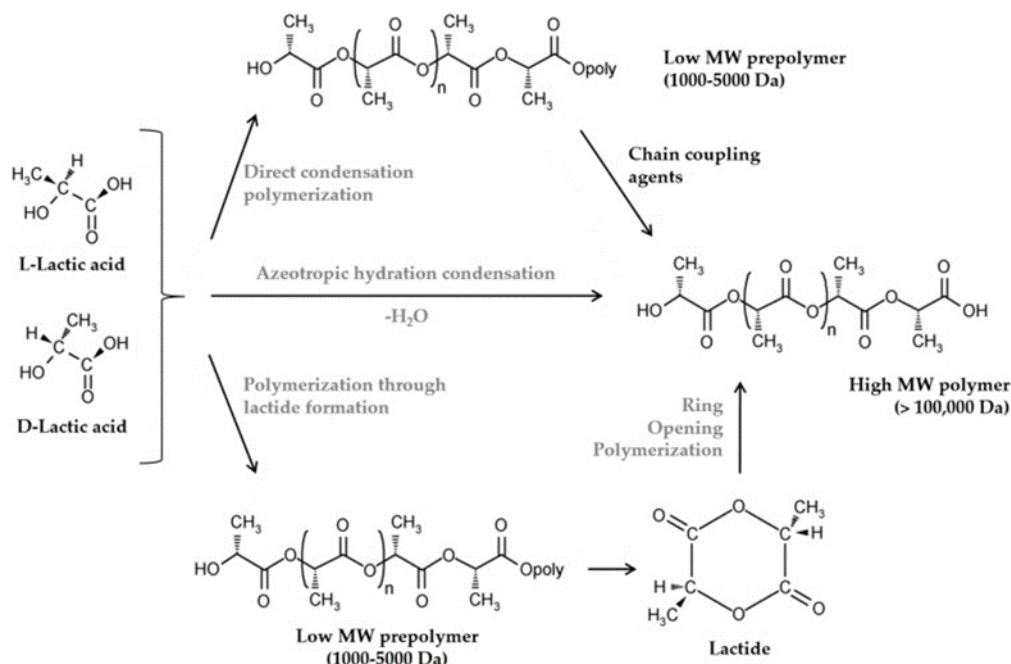


Figure 1 Different routes to produce PLA. [4]

PLA is to be used in packaging and consumer products. Since PLA can be composted and made from renewable resources, it has been considered as possible solution to the issue of the disposal of solid waste and reducing the use of plastics generated from petroleum. Despite the fact that typical converting equipment can process PLA with only little modifications, some applications require polymers [4].

There are three possible stereochemical forms of lactide: L-, D-, or both L- and D-Lactide (meso-lactide), each with its specific melting characteristics. Water, ethanol, methanol, and aliphatic hydrocarbons are insoluble in PLA. However, it is soluble in hazardous substances like chloroform, heated benzene, acetonitrile, acetone, ethyl acetate, and dichloromethane. Its stereochemistry and molecular weight determine the range of its half-life for degradation, which is between six months and two years [9].

2.2 Polybutylene Succinate (PBS)

PBS is a biopolymer that is derived from the poly-condensation of succinic acid and 1,4-butanediol (BDO). It offers manufacturers of plastics a potentially useful component for the construction of biopolymer compounds.

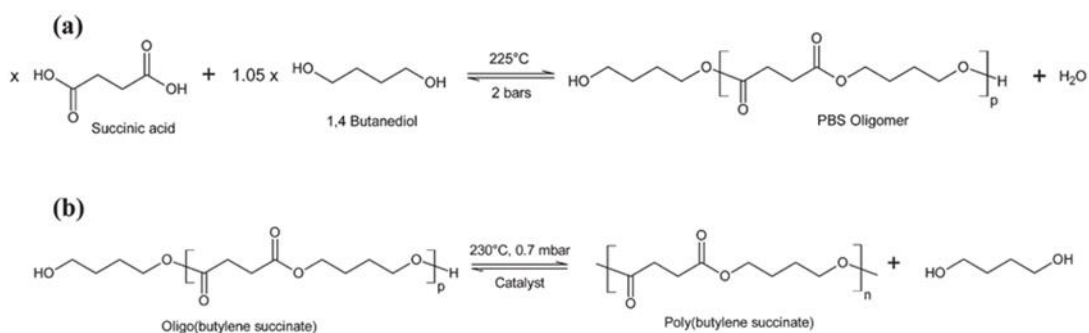


Figure 2 Schematic representation of PBS synthesis from SA and BDO. (a) esterification, (b) transesterification [10].

PBS is a type of crystalline polyester that has a melting point that is higher than 100 degrees Celsius and is necessary for use in high-temperature applications. Temperatures as high as 200 degrees Celsius can be reached during processing, depending on the conversion method used. In order to prevent chain scissions, decomposition, and enhanced fluidity, the residence time needs to be kept short when the temperature is high. In Table 1, the mechanical properties of polybutylene sulfide (PBS) and polybutylene sulfonic acid (PBSA), a typical co-polymer of PBS that also contains adipic acid, are compared to those of several biopolymers and conventional polymers derived from petroleum. When compared to other plastics that are often derived from petroleum, PBS most closely resembles LDPE in terms of its qualities [11].

Table 1 Comparison of exemplary physical properties of PBS compared to other (bio based) polymers.

	PBS	PBSA	PLA	HDPE	LDPE	PS	PP
Glass transition temperature (°C)	-32	-45	55	-120	-120--40	105	-5
Melting point (°C)	114	96	140-180	129	110	Amorphous	163
Heat distortion temperature (°C)	97	69	55	82	49	95	110
Tensile strength (MPa)	34	19	66	28	10	46-60	33
Elongation at break (J/m, %)	560	807	4	700	300	3-4	415
Degree of Crystallinity (%)	34-45	20-30	0-40	69	49	0	56

PBS is resistant to chemicals and high temperatures, as well as melt processing and biodegradation. PBS is a versatile polymer that may be molded into injection-molded products in the plastics industry as well as melt-blow, multifilament, thermoforming, flat, and split yarn in the textiles industry.

2.3 Ethylene-Propylene Diene Monomer (EPDM)

EPDM is a copolymer containing ethylene, propylene, and a small percentage (3 to 9 percent) of non-link diene monomers that give cross-linking sites for vulcanization:

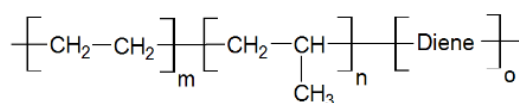


Figure 3 Typically, dicyclopentadiene, ethylidene norbornene, or 1,4 hexadiene is the diene. These terpolymers may be vulcanized using conventional methods.

EPDM elastomers have excellent resistance to high temperatures, chemicals, ozone, and the aging effects of weathering. They also offer excellent electrical insulation, compression set, and low-temperature qualities, although it is unlikely that they would be used in applications requiring physical strength. In terms of its resistance

to chemicals, EPDM can withstand polar fluids, hot water, and steam at temperatures up to 200 degrees Celsius (in the absence of air). It's safe to say that EPDM are the most water-resistant rubbers on the market. However, they are not compatible with hydrocarbon fuels or solvents, mineral or synthetic diester lubricants, or mineral or synthetic diester lubricants. In addition to this, their resistance to flame is quite poor [12].

2.4 Polymers Blends

A polymer blend is a mixture of 2 or more polymers through various forms of blending. Whether mixed melting or mixed with solvent, etc. The polymer blends can be divided into 3 main groups according to the mixing compatibility: 1. Miscible polymer blends are polymer blends that are compatible at all molecular levels. And homogeneous. 2. Partial polymer blends are polymer blends that are compatible in some parts. 3. Immiscible polymer blends are incompatible polymer blends. In most cases, most polymer blends are classified as Immiscible polymer blends using thermodynamic principles used to explain by the equation used to describe according to Equation (1)

$$\Delta G_M = \Delta H_M - T\Delta S_M \quad (1)$$

Where ΔG = change in free energy

ΔH = change in enthalpy

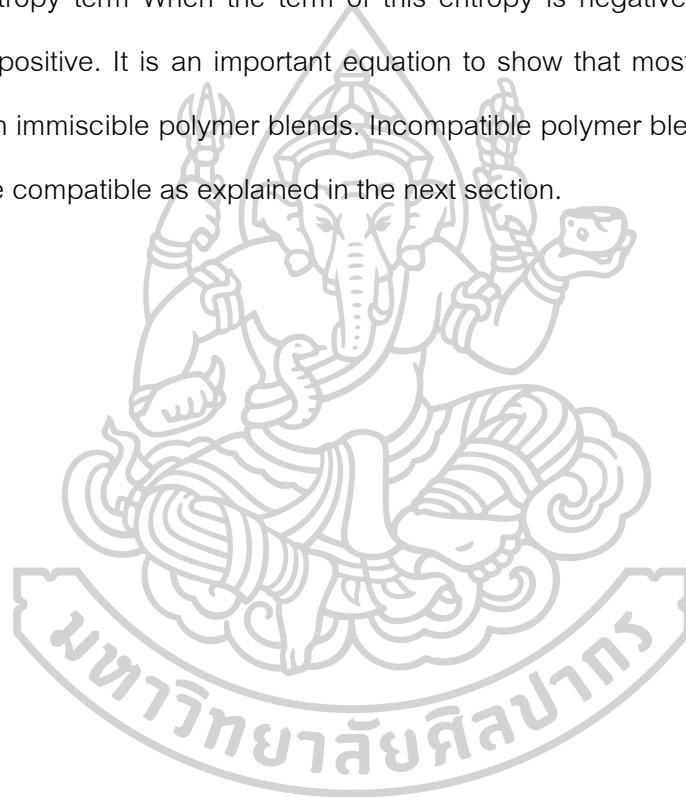
ΔS = change in entropy

T = absolute temperature

M = mixing.

If the energy of mixing is positive, then the polymer blend is immiscible polymer blends. And if the energy of mixing is Negative means that the polymer blends are Miscible polymer blends [13].

In most cases, the polymer blends have a positive free energy change due to the molecular chain of polymers. Most Users with a high molecular weight make chains of polymer is very long. Therefore, greatly limits the movement of the chain, resulting in a negative entropy term When the term of this entropy is negative, the thermodynamic equation is positive. It is an important equation to show that most polymer blends are blended with immiscible polymer blends. Incompatible polymer blends have methods to can be more compatible as explained in the next section.



2.5 Thermoforming Process

Thermoforming is a technique adopted from the field of metallurgy. As indicated in Figure 4, a plastic sheet is heated until it softens and then shaped into the shape of a mole by applying external air pressure or by drawing a vacuum between the sheet and mole. Ancient Egyptian artisans who softened tortoise shells into various shapes may have been the first thermoforms. However, the current thermoforming business did not begin until 1938, with the creation of blister packaging from cellulose acetate sheet. Today's thermoforming applications in the plastics sector extend to the mass production of plastic cups to manufacture plastic bed covers for half-ton pickup trucks.

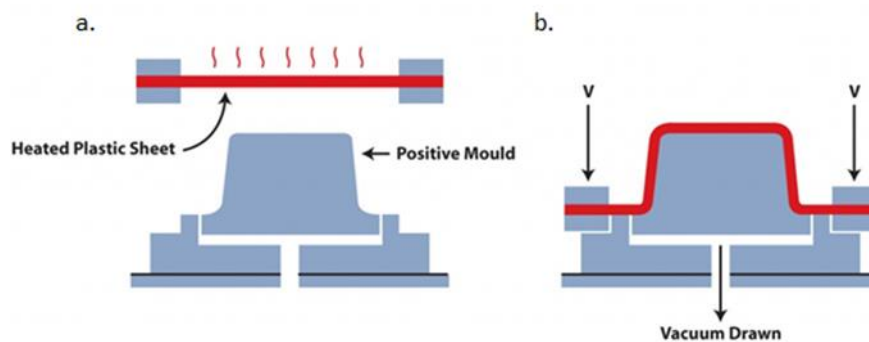


Figure 4 Vacuum forming procedure. a. Heating the flat sheet. b. The space between the softened sheet and the mold is evacuated, forcing the sheet to conform to the shape of the mold. [14].

2.6 Mechanical Analysis

2.6.1 Universal tensile testing

A tensile test can be used to examine the mechanical properties of a material, in which a tensile force is applied at both ends of a specimen of the material. This test is performed to compute or quantify a material's tensile strength and any other tensile

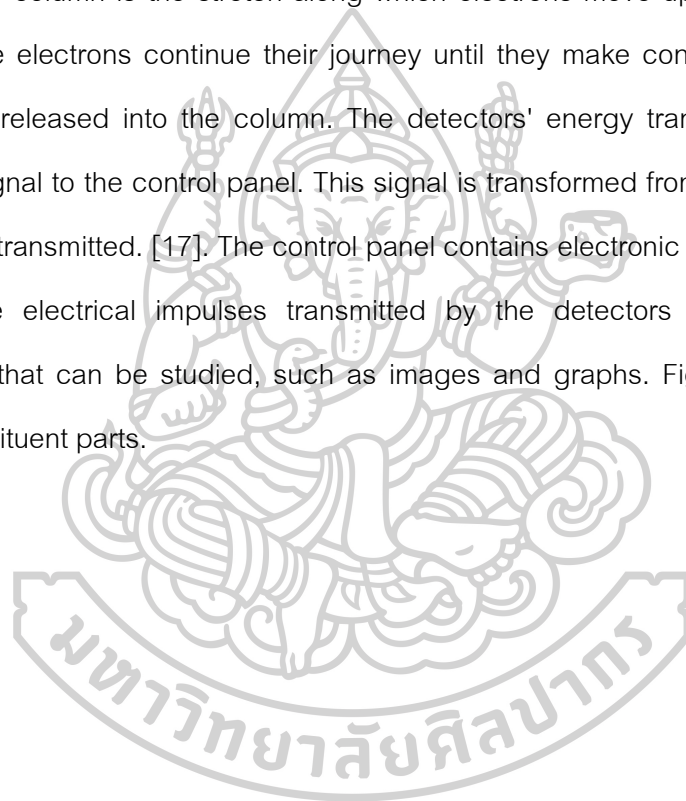
properties [15]. The objective of this test is to compare different materials and methodologies. The majority of the specimens have a dumbbell form.

2.6.2 Impact testing

The amount of energy that is consumed up until the point of failure under rapid loading conditions can be measured using impact tests. These tests are performed with the aim of determining how strong a material is. When it comes to impact tests, there is a wide variety of different choices accessible to choose from. The well-known Izod and Charpy test is one of them. In this test, a weight that resembles a hammer is used to strike a specimen, and the amount of energy needed to break the specimen is determined based on the amount of kinetic energy lost by the hammer. There is also a test known as the falling ball or dart test. The amount of energy that must be exerted in order to fracture the object is determined by taking into account both the mass of the ball and the depth from which it is dropped. This information is then used in the test. The region underneath the stress-strain curve can also be utilized in high-speed tensile testing in order to obtain values of the material's impact strength. The information on deformation and fracture processes can be gleaned from instrumented impact testing, which provides a comprehensive report of the load that was applied to the specimen throughout the entirety of the impact event [16]. This information can be used to gain insight into the processes of deformation and fracture.

2.7 Scanning Electron Microscopy (SEM)

The scanning electron microscope, frequently abbreviated SEM, consists of two essential parts: the column and the cabinet (Figure 5). The column is the extent down which the electrons travel after their emission until they reach the sample, where the detectors will capture the scattered signals created by the electrons' contact with the sample. The column is the stretch along which electrons move up until they reach the sample. The electrons continue their journey until they make contact with the sample after being released into the column. The detectors' energy transducers transmit an electrical signal to the control panel. This signal is transformed from the signal type that was initially transmitted. [17]. The control panel contains electronic components that can quantify the electrical impulses transmitted by the detectors and turn them into information that can be studied, such as images and graphs. Figure 5 illustrates the SEM's constituent parts.



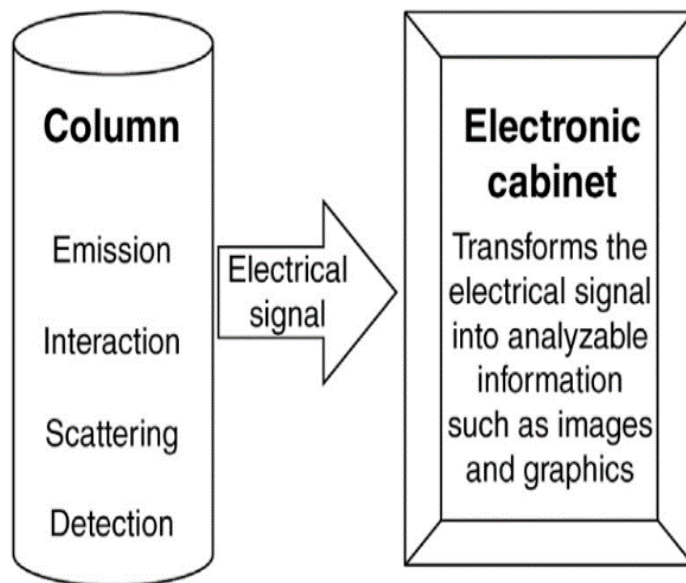
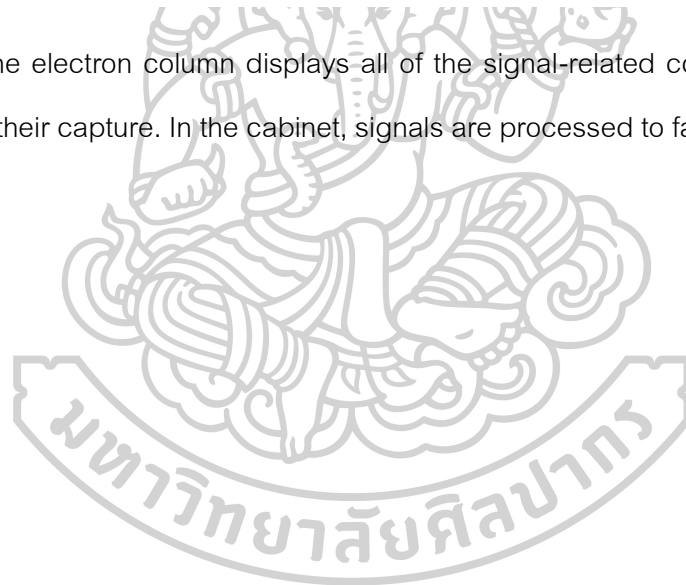


Figure 5 The electron column displays all of the signal-related components from their emission to their capture. In the cabinet, signals are processed to facilitate display [17].



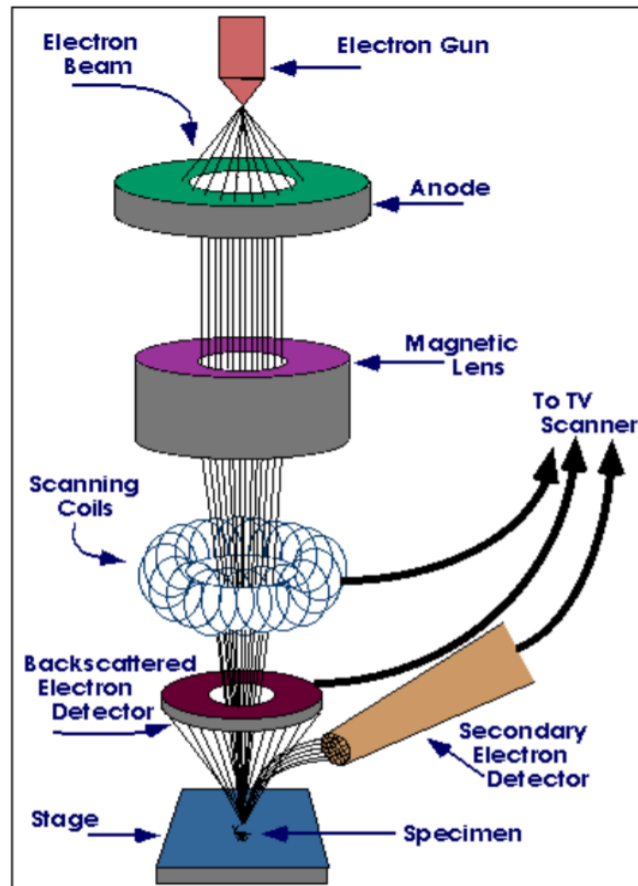


Figure 6 Schematic illustrations the components of scanning electron microscopes [18].

An electron beam is used to trace a sample in a raster pattern while a scanning electron microscope (SEM) is used to obtain detailed surface information. The procedure starts with an electron gun that fires a stream of high-energy electrons down a column and into a set of electromagnetic lenses. These lenses are referred to as solenoids, and they take the form of tubes wrapped in coils. These adjustments generate oscillations in the voltage, which in turn increases or decreases the speed at which the electrons come into contact with the specimen surface. These modifications are made to the coils so that the incident electron beam can be focused on the sample. The SEM operator has the ability to change the beam to control magnification and determine the surface area that is to be scanned, both of which are controlled by the computer. The beam is focused onto the stage, which is subsequently occupied by a

solid sample. Before being placed in the vacuum chamber, the vast majority of samples call for some sort of pretreatment. Sputter coating, which is used for non-conductive materials, and dehydration, which is used for most biological specimens, are the two types of preparation methods that are utilized the most frequently prior to scanning electron microscopy (SEM) analysis. In addition, it is necessary for each sample to be able to withstand the low pressure that is present within the vacuum chamber. The rate of acceleration of the incident electrons, which carry considerable quantities of kinetic energy before being focused onto the sample, is what determines the nature of the interaction that occurs between the incident electrons and the surface of the sample. Electrons of high energy are emitted from the surface of the sample when it is struck by incident electrons and the incident electrons come into contact with the sample. The scatter patterns that are produced as a result of the contact provide information about the size, shape, and texture of the sample as well as its composition. A wide variety of detectors, such as secondary and backscattered electron detectors, as well as x-ray detectors, are utilized in the process of attracting various forms of scattered electrons. Backscatter electrons are incidental electrons that are reflected backwards, and they give data on the composition of images relevant to the identification of elements and compounds. A backscatter detector can be used to gather topographic information; however, the accuracy of this information is compromised. Crystalline structures, in addition to the orientation of minerals and micro-fabrics, are established through the use of diffracted backscatter electrons. X-rays that are emitted from below the surface of the sample can provide information regarding the elements and minerals present. Images in three dimensions and in black and white are produced by SEM. Although it is not as powerful as its TEM counterpart, the intense interactions that take place on the surface of the specimen provide a greater depth of view, higher-resolution, and ultimately, a more detailed picture of the surface [19]. Image magnification can be as high as 10

nanometers, and while it is not as powerful as its TEM counterpart, it does provide a more detailed picture of the surface.

2.8 Thermal Analysis

2.8.1 Differential Scanning Calorimetry (DSC)

The differential scanning calorimeter, or DSC, is the method of choice when doing thermal analyses on polymeric materials. When a substance and a reference material are put through a controlled temperature program, it measures the difference in the amount of energy that is put into each of the two substances. Changes in enthalpy or specific heat are common to virtually all chemical and physical processes; hence, the applicability of differential scanning calorimetry (DSC) to condensed phase systems is practically limitless [20]. The procedure of measuring it is quantitative, and the enthalpy change those results is often a linear function of the reaction coordinate. Figure 7 illustrates a DSC peak that is either endothermic or exothermic. Since a DSC measurement provides the rate of change in enthalpy, the total heat of reaction can be determined by calculating the area between a DSC curve and its extrapolated baseline. The reaction fraction can be calculated by dividing the fractional area by the total area to obtain the answer. The rate of reaction can be determined by calculating the amplitude of the difference between the baseline and the DSC curve [21].

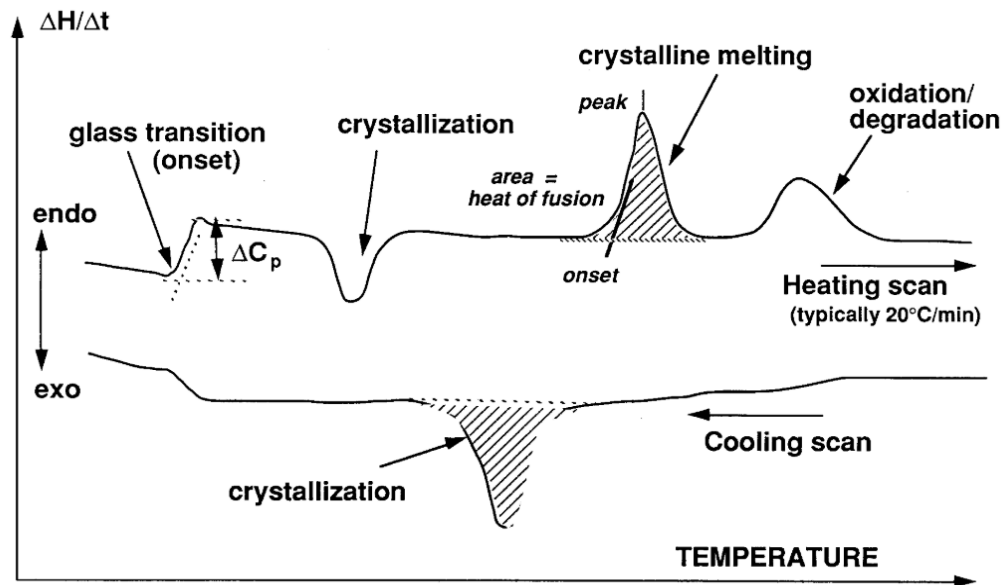


Figure 7 Illustrates typical polymer DSC thermograms [22].

Figure 7 describe the characteristics of thermal changes in the heating test (heating scan). Will find the characteristic of the heat change is T_g peak melting temperature and the area under the graph represents the energy of enthalpy. To melt crystals (crystalline melting) When the temperature is rising, the thermal decomposition temperature will be found (oxidation or degradation) while providing cooling (cooling scan). Will find the peak position of the crystallization temperature and the area under the graph represents the energy of enthalpy. In the process of crystallization, the findings of a study carried out with a DSC can be translated into a percentage of crystal content that can be estimated using the equation below (2)

$$X_C = \left[\left(\frac{\Delta H_m}{\Delta H_m^0} \right) \times \frac{100}{W} \right] \quad (2)$$

When W is the proportion of polymer matrix in the composite material

ΔH_m is the amount of heat required to anneal the polymer matrix

ΔH_m° is enthalpy of annealing a polymer that is 100% crystalline

2.8.2 Thermogravimetric Analysis (TGA)

Thermogravimetric analysis, or TGA for short, is one of a family of thermal analysis techniques that can be used to analyze a wide range of different types of materials. The thermogravimetric analysis, or TGA, is a technique that analyzes the amount and rate (velocity) of change in the mass of a sample as a function of temperature or time in an environment that is under controlled conditions. The primary purposes of the measurements are to ascertain the thermal and oxidative stabilities of the material in addition to determining the compositional qualities of the substance. Materials that experience either a loss or gain in mass as a result of decomposition, oxidation, or the loss of volatiles can be analyzed using this technique (such as moisture). The study of polymeric materials, such as thermoplastics, thermosets, elastomers, composites, films, fibers, coatings, and paints, can benefit from it. This includes all of the aforementioned materials. TGA measurements give useful information that can be used to select materials for specific end-use applications, anticipate product performance, and enhance product quality [23]. Such information can also be used to improve product quality.

2.9 Chemical Structure and Interaction

2.9.1 Fourier-Transform Infrared Spectroscopy (FTIR)

Infrared spectroscopy using the Fourier transform, often known as FTIR, is a method that may be used to acquire an infrared spectrum of a substance's absorption, emission, photoconductivity, or Raman scattering. This method can be used on solids, liquids, or gases. FTIR spectrometers are capable of concurrently collecting spectral data over a broad range of wavelengths. A dispersive spectrometer, which measures intensity over a limited range of wavelengths at once, has a substantial disadvantage in comparison to this method, which measures intensity over a wider range of wavelengths simultaneously. Infrared spectroscopy has been given new uses as a result of the

development of FTIR, which has rendered dispersive infrared spectrometers mostly extinct (save for occasionally in the near infrared). FTIR is used to the nanofibrous scaffolds in order to examine the interactions between antimicrobial agents and polymers. In this method, a total of one percent by weight of the sample, in relation to the potassium bromide (KBr) disc, is combined with dry KBr. Before being compacted into a KBr disc using a hydraulic press at a pressure of 10,000 psi, the mixture is first reduced to a powder using an agate mortar to get a finer consistency. Using IR solution software, each KBr disc is scanned at a rate of 4 millimeters per second with a resolution of 2 centimeters throughout a wavenumber range of 400–4000 cm^{-1} [24].

2.10 Crystal Structure

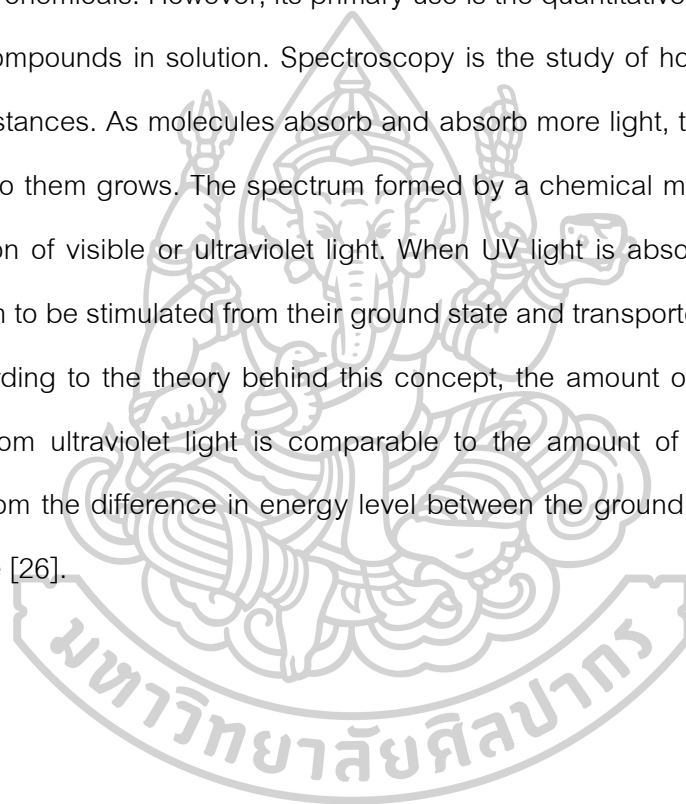
2.10.1 X-Ray Diffraction (XRD)

Analysis is a technique aimed to offer more information on crystalline substances, such as identification and quantification of crystalline phases. This is a helpful instrument when attempting to positively identify a contaminant or corrosion product, as well as for identifying foreign phases for purity tests of crystalline powders [33]. In XRD analysis, a focussed X-ray beam is fired at a specified angle of incidence at the sample. Depending on the crystal structure (distances between atoms) of the sample, X-Rays deflect or "diffract" in various ways. The locations (angles) and intensities of the X-Rays that have been diffracted are measured. Each substance has an own diffraction pattern. To identify a chemical, the sample's diffraction pattern is compared to a database of known patterns. In addition to identifying crystalline phases, the peak forms and intensities acquired during XRD analysis may be utilized to determine the % crystallization and crystalline size [25]. The identification of crystalline phases for a wide variety of powders and thin-film materials is the principal application of XRD analysis. This involves the study of corrosion products, ceramics, clays, oxide or nitride coatings, and a number of other substances. XRD can distinguish between compounds with the same components but different characteristics, such as Fe_2O_3 and Fe_3O_3 , because it

is structure-based. Frequently, it is also possible to establish the approximate concentrations of each crystalline phase [22].

2.11 Ultraviolet-Visible Spectroscopy (UV-vis)

In the realm of analytical chemistry, ultraviolet-visible spectroscopy is widely acknowledged as a crucial tool. Due to its usage in qualitative chemical analysis and identification, it is one of the most commonly employed techniques in laboratories dealing with chemicals. However, its primary use is the quantitative study of organic and inorganic compounds in solution. Spectroscopy is the study of how light interacts with various substances. As molecules absorb and absorb more light, the quantity of energy accessible to them grows. The spectrum formed by a chemical molecule as a result of its absorption of visible or ultraviolet light. When UV light is absorbed by electrons, it causes them to be stimulated from their ground state and transported to a higher energy state. According to the theory behind this concept, the amount of energy that can be extracted from ultraviolet light is comparable to the amount of energy that can be extracted from the difference in energy level between the ground state and the higher energy state [26].



CHAPTER 3

LITERATURE REVIEWS

Yokohara, Okamoto and Yamaguchi [27] studied the effects of the shape of dispersed particles on the thermal and mechanical properties of polymer blends were studied and compared with the properties of blends containing spherical particles of PBS in a continuous PLA phase. These blends had a high degree of crystallization and enhanced the cold crystallization in the heating process.

Yokohara and Yamaguchi [28] studied the properties and structures of the blends between PLA and PBS. The thermal testing result showed that the immiscible phase structure and phase separation of PLA/PBS blends. At the ratio of PLA/PBS (80/20) found that the particle PBS dispersed on PLA matrix continuous phase. PBS act as nuclei for PLA crystallization because the crystallization peak is clearly detected around at 90 °C demonstrating that PBS droplets act as nucleating entities for PLA. The occurrence of PBS droplet corresponds to the crystal characterization of blends with the optical microscope found that PLA and PBS would not be able to see the crystal at a cooling rate of 2 °C/min. Obviously formed crystals when added the PBS in PLA.

Bitinis, et al. [29] studied the shape as well as the physical qualities of mixes of natural rubber with polylactic acid (PLA). By adding 10 weight percent more of the NR component, it was discovered that the elongation at break of PLA/NR blends rose from 5 to 200%. The fracture surfaces of the PLA/NR mixes are depicted in Figure 8. With a rise in NR concentration from 5 to 20 wt%, it was discovered that the droplet size of NR in PLA matrix increased from 1.15 to 2.03 μm . This suggested that the immiscibility in the PLA/NR blends was brought about by the larger droplets and the low dispersed phase.

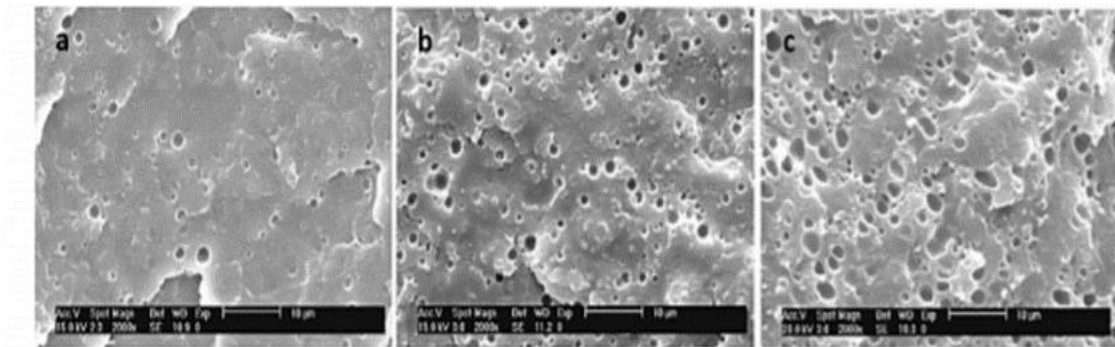


Figure 8 Morphology of NR droplet size in PLA/NR blends at different NR concentrations (a) 5 wt%, (b) 10 wt% and (c) 20 wt%. [29]

Dong Hyup Park, et al. [30] studied the hydrolysis degradation of PP/EPDM/PLA ternary blends was researched in the presence of distilled water at 85 °C, and subsequently the changes in their mechanical characteristics were tested. It was discovered that the tensile strength of blends of PP, EPDM, and PLA with weight fractions of 0.5, 0.6, and 0.7 percent PLA dropped significantly until the hydrolysis period reached three days. (Figure 9) After that, there was no change in the tensile strength. The tensile strength of the blends rapidly falls till the hydrolysis time reaches three days as the PLA concentration decreases from 0.1 to 0.2 to 0.3 and 0.4 weight fractions of PLA. After that, there was no change in the tensile strength as a function of the hydrolysis time.

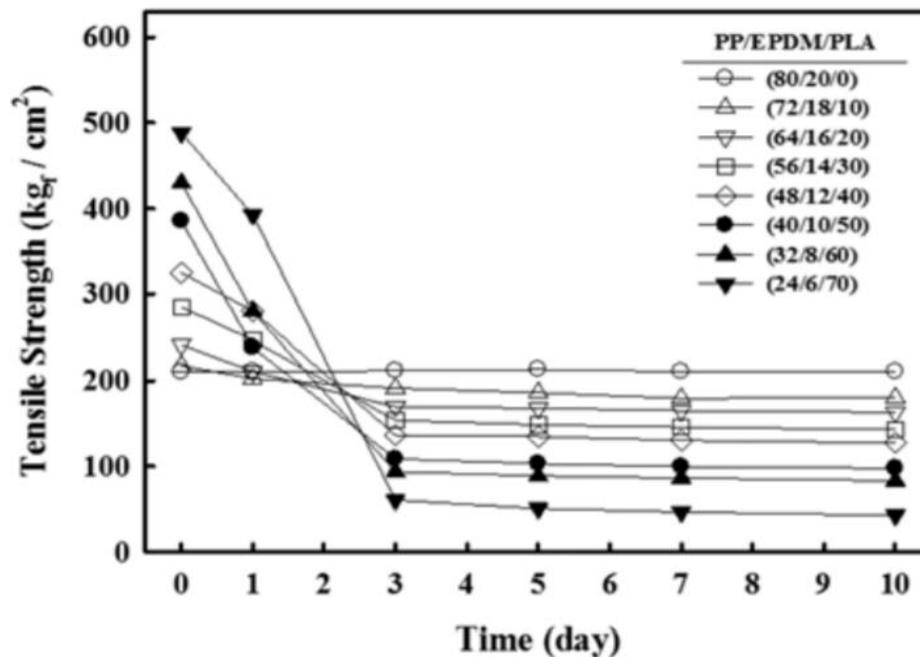


Figure 9 Shows tensile strength of the PP/EPDM/PLA blends with. PLA content and hydrolysis time. [30]

Yun Huang, et al. [31] studied the effects of applying dicumyl peroxide to PLA/NR composites. It was discovered that when DCP undergoes internal mixing, heating causes it to break down into radicals. These radicals will then attack PLA or NR chains to generate more radicals, which will then pair and cause crosslinking to take place. (Figure 10) The fracture of PLA, PLA that has been treated with 0.5 weight percent DCP, PLA/NR blend, and PLA/NR blend that has been treated with 2 weight percent DCP can be shown in Figure 11 of the scanning electron microscopy (SEM) image. When pure PLA is broken, the surface of the crack is uniform throughout. The surfaces of Figure 11 b and d are extremely rough, almost as if there were some kind of particle covering on them.

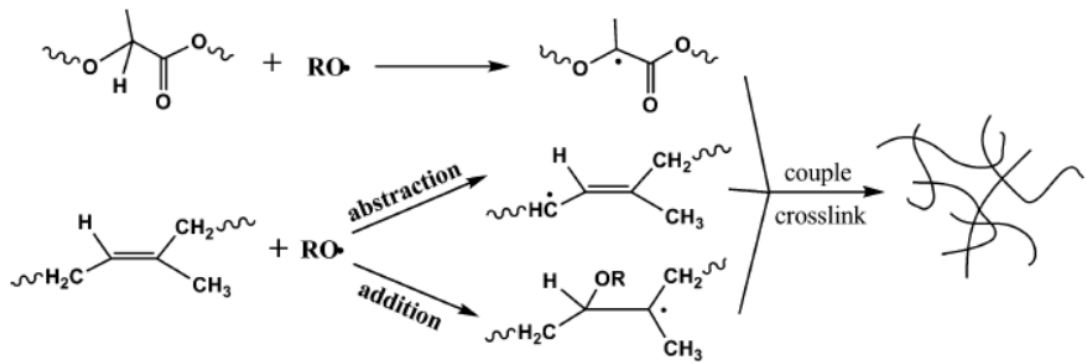


Figure 10 Reactions that are initiated by DCP, producing macromolecular free radicals, include NR and PLA (RO is for cumyloxy radical).[31]

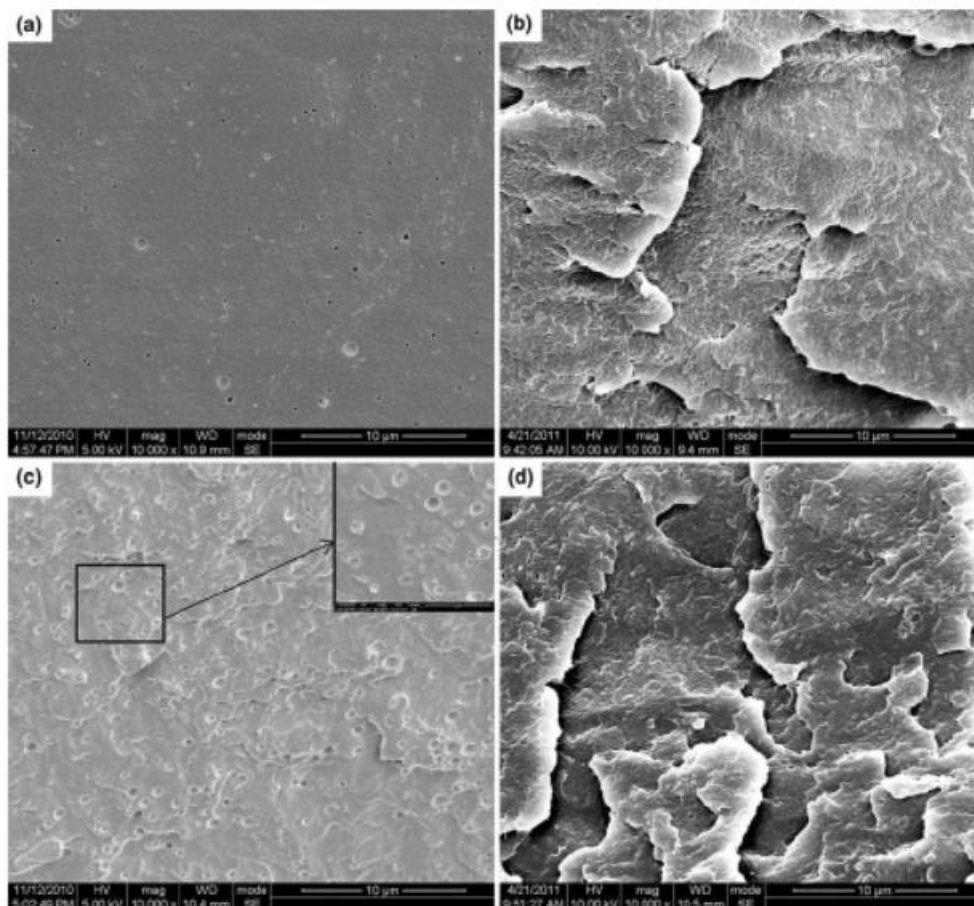
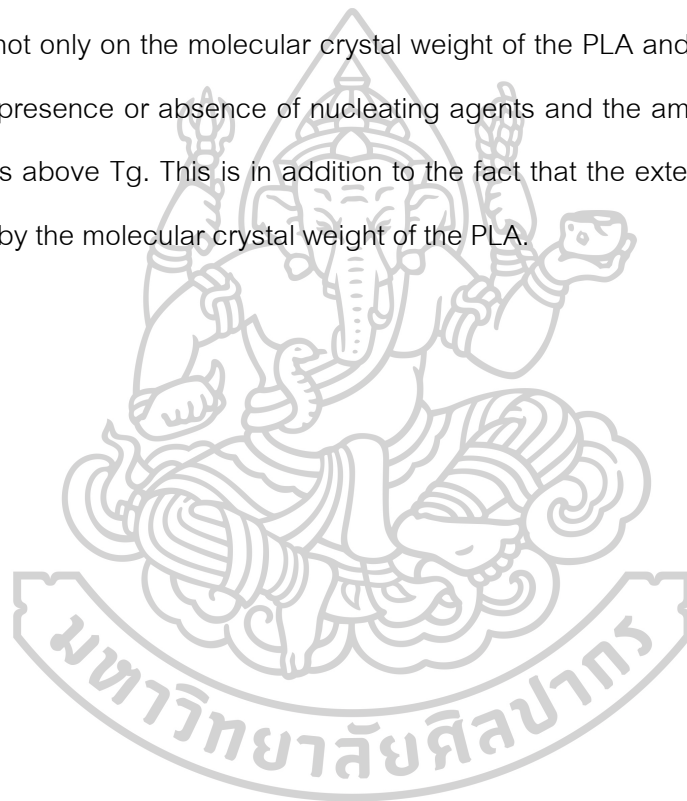


Figure 11 SEM images of freeze-fracture surface of a PLA, b 0.5 wt% DCP/PLA, c PLA/NR and d 2 wt% DCP/PLA/NR. [31]

Bigg. [32] studied the molecular weight of PLA polymers can have an effect on the behaviors of thermoforming. They reported that at a thermoforming temperature of 75 °C, PLA copolymer with a molecular weight of 268,000 cannot be thermoformed to provide satisfactory definition because the molecular weight was too high. Additionally, due to the low molecular weight, copolymer with a Mw of 120,000 is unable to be thermoformed correctly. This is because the low molecular weight led to tearing at corners and areas where deep draws took place. The extent of crystallization is dependent not only on the molecular crystal weight of the PLA and the type of PLA, but also on the presence or absence of nucleating agents and the amount of time spent at temperatures above T_g. This is in addition to the fact that the extent of crystallization is determined by the molecular crystal weight of the PLA.



CHAPTER 4

METHOD OF RESEARCH

4.1 Materials

4.1.1. Poly(Lactic Acid), (PLA)

In this study, PLA was utilized, and its commercial name is Ingeo biopolymer 2003D. The melt flow index for this material was 6.0 g/10 minutes, and its specific gravity was 1.24 g/cm³. Nature Works LLC in the United States manufactured the PLA. The temperature at which PLA melted was around 210 °C. Figure 12 depicts the PLA pellets that were used.



Figure 12 PLA commercial name Ingeo Biopolymer 2003D.

4.1.2. Poly(Butylene Succinate), (PBS)

This study made use of PBS that had a melt flow index of 5.0 g/10 min and a density of 1.26 g/cm³. PBS was developed in the United States by Nature Works LLC. Figure 13 depicts the PBS pellets in their entirety.



Figure 13 Poly(butylene succinate), (PBS).

4.1.3. Ethylene-Propylene Diene Monomer (EPDM)

EPDM with the ethylene content of 70.0 wt%, ethylidene norbornene (ENB) content of 0.5 wt% and propylene content of 29.5 wt% was produced by Dow Chemical Company under the Commercial name of "NORDEL IP 3745P". EPDM with the specific gravity of 0.88 g/cm^3 . The EPDM pellets is shown in Figure 14.



Figure 14 Ethylene propylene diene monomer rubber (EPDM rubber).

4.2 Preparation of Materials

4.2.1 Preparation of PLA/PBS blends.

PLA and PBS were dried before combining. Both PLA and PBS were dried in an oven at 80 °C for four hours each. The temperatures were kept constant during the drying process. Melt blending was used to prepare PLA/PBS blends in an internal mixer, as illustrated in Figure 15, at a temperature of 180 °C and a rotor speed of 70 revolutions per minute for a period of 13 minutes. The weight percentages of the PBS were 10, 20, and 30.

4.2.2 Preparation of PLA/PBS/EPDM ternary blends.

PLA, PBS and EPDM were dried before blending. PLA was dried in an oven at 80 °C for 4 hours and PBS was dried in an oven at 80 °C for 4 hours. PLA/PBS/EPDM ternary blends were prepared by melt blending in an internal mixer as shown in Figure 15 at 180 °C and rotor speed of 70 rpm for 13 min. The PBS contents were 5, 10 and 15 wt% and the EPDM contents were 5, 10 and 15 wt%.

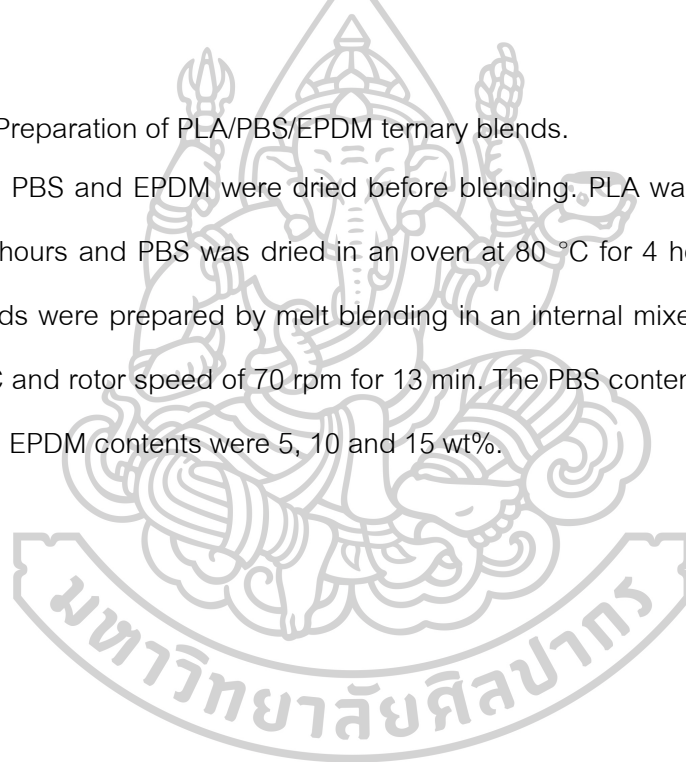


Table 2 Composition of the prepared binary and ternary blends.

Sample	PLA wt%	PBS wt%	EPDM wt%
PLA	100	-	-
PBS	-	100	-
EPDM	-	-	100
PLA/PBS	90	10	-
PLA/PBS	80	20	-
PLA/PBS	70	30	-
PLA/PBS/EPDM	80	15	5
PLA/PBS/EPDM	80	10	10
PLA/PBS/EPDM	80	5	15
PLA/EPDM	80	-	20



Figure 15 Internal mixer.

4.3 Sample Preparation

4.3.1 Dog bone or Dumbbells shape

Before molding in compression molding as shown in Figure 16 polymer blends were dried in an oven at 100 °C for 1 hours for reject moisture. Dumbbells shape for tensile test was done by compression molding at 180 °C, 5,000 psi for 15 min.

4.3.2 Bar shape

Before molding in compression molding as shown in Figure 16 polymer blends were dried in an oven at 100 °C for 1 hours for reject moisture. Bar shape for impact test was done by compression molding at 180 °C, 5,000 psi for 15 min.

4.3.3 Film or sheet shape

Before molding in compression molding as shown in Figure 16 polymer blends were dried in an oven at 100 °C for 1 hours for reject moisture. Film shape for DSC, TGA, XRD and UV test was done by compression molding at 180 °C, 5,000 psi for 15 min.

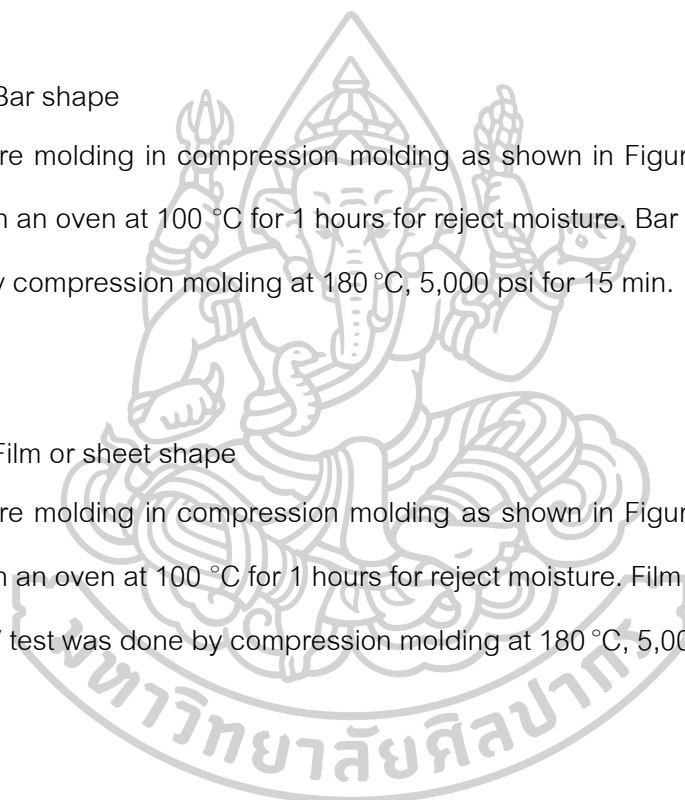




Figure 16 Compression molding machine

4.4 Sample characterization

4.4.1 Tensile test

Tests of tensile strength were carried out in accordance with ASTM D 638 utilizing a universal tensile testing machine (EZ Test, EZ-LX/EZ-SX series), as illustrated in Figure 17. Tensile characteristics were determined using a crosshead speed of fifty millimeters per minute and a temperature of room temperature. The specimens in the form of dumbbells, which were present in all of the blending samples, were stretched at a steady speed until they broke. The materials were put through their paces in order to ascertain their qualities, such as their Young's modulus, tensile strength, and elongation at breakage, amongst others. The values that were obtained were representative of the averages of the data obtained from five separate samples.



Figure 17 Universal tensile testing machine.

4.4.2 Impact test

Tests of Izod's resistance to impact were carried out at room temperature in accordance with ASTM D 256. As can be seen in figure 18, the impact tester, model XJC-25D, was put to use with a pendulum rated at 4 J. The compression molding method was used to prepare the bar samples. The specimens with the notches were the ones used for the test. The figures for the Izod impact strength were determined by taking the average of a set of five different specimens.



Figure 18 Impact testing machine.

4.4.3 SEM observation

The scanning electron microscopy (SEM) technique was utilized to investigate the morphology of tensile fractured specimens of PLA, PLA/PBS blends, PLA/PBS/EPDM ternary blend, and composites. The scanning electron microscope (SEM) was utilized in order to investigate the fracture surface's texture as well as the dispersion of the minor phase within the mixes. The scattered electron image (SEI) mode was utilized throughout the SEM analysis. Before the measurement, the broken surfaces of each and every blending sample were sputter-coated with a very small layer of gold using an

electrostatic sputtering technique to increase their conductivity. Figure 19 depicts the instrument that makes up the MIRA3 FEG-SEM, which is an acronym for "A Flexible Scanning Electron Microscope."



Figure 19 MIRA3 FEG-SEM (A Flexible Scanning Electron Microscope)

4.4.4 Differential scanning calorimetry, (DSC)

A DSC was used in order to get a better understanding of how PLA mixes behave thermally (SDT 0600, TA Instrument). The polymer mix films were made using compression molding as the preparation method. Aluminum tins were used to hold the specimens, each of which had a mass ranging from 6 to 8 mg. The glass transition temperature (T_g), the melting temperature (T_m), and the heat of fusion (H_m) were among the thermal parameters that were measured and analyzed. The test was performed in an environment containing nitrogen at temperatures ranging from fifty to

two hundred degrees Celsius. The DSC thermograms were taken at a heating rate of 10 °C per minute.

4.4.5 Thermogravimetric analysis, (TGA)

The thermal stability of the sample was analyzed using TGA (STD Q600), and polymer blends were used as the test material. As can be seen in Figure 20, this instrument may be found at Chulalongkorn University's center of excellence on catalysis and the Catalysis reaction. The polymer films that were produced using the compression molding procedure were sliced up into smaller pieces, and each scan utilized anywhere between 5 and 10 mg of polymer samples. After that, the samples were heated in a nitrogen atmosphere from 50 °C to 600 °C at a rate of 10 °C per minute. As a function of temperature, the thermal decomposition of the samples, expressed as a percentage of weight loss, was monitored and recorded.



Figure 20 Thermogravimetric analysis, (TGA)

4.4.6 Dynamic mechanical analyzer (pyris diamond DMA)

Utilizing the dynamic mechanical analyzer (DMA), all polymer samples' dynamic mechanical characteristics were investigated. The tests were performed at a frequency of 1 Hz at temperatures ranging from 30 to 160 °C. With a twin cantilever in bending mode, the measurements were conducted. By use of compression molding, rectangular blend specimens (dimensions 1.51050 mm³) were created. As a function of temperature, the viscoelastic properties storage modulus (E'), loss modulus (E''), and mechanical damping parameters (tan) were measured.



4.4.7 X-Ray diffractometer analysis (XRD)

X-ray diffraction (XRD analysis) is a unique technique for determining the crystallinity of polymer mixes containing PLA. The X-Ray Diffractometer (Bruker AXS Model D8 Discover) was placed at Chulalongkorn University's center for scientific and technical research equipment. The polymer films generated by the method of compression molding were cut into little 3x3 cm² pieces for use in each scan. XRD analysis relies on constructive interference between monochromatic X-rays and a crystalline specimen: The X-rays are produced by a cathode ray tube, filtered to produce monochromatic radiation, collimated to concentrate, and focused on the sample. The interaction of light rays with the sample generates constructive interference (and a diffracted ray) under Bragg's Law ($n = 2d\sin$), 0.154 nm wavelength, 40 kV, and 40 mA operation. A crystalline sample was scanned in the 2 range from 1 °C to 10 °C with a scanning step of 0.02° and a scanning rate of 0.5 sec/step to get the X-ray diffraction angle and the lattice spacing. A diffractogram is the outcome of an XRD investigation, displaying the intensity as a function of the diffraction angles. XRD is illustrated in Figure 21.

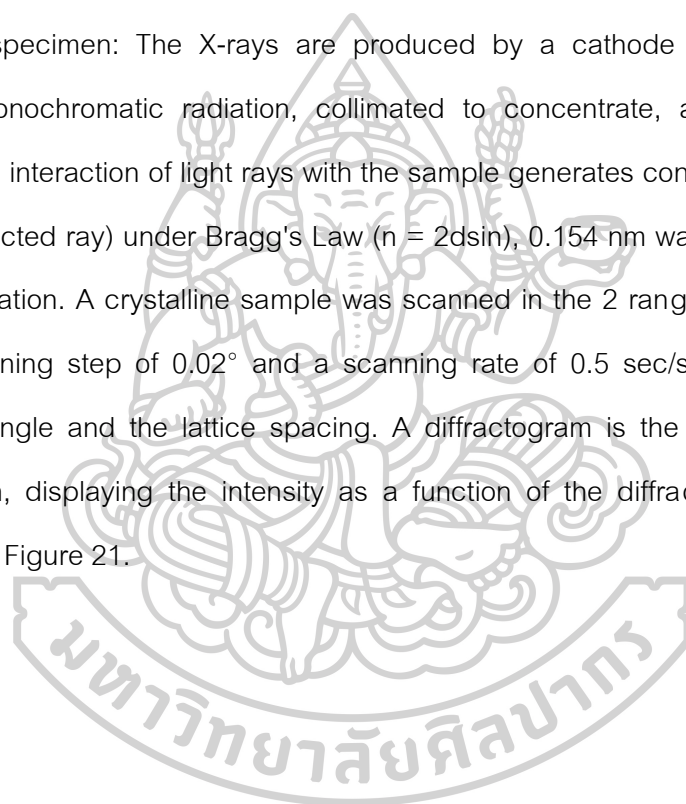




Figure 21 X-Ray Diffractometer (Bruker AXS Model D8 Discover)

4.4.8 Fourier-Transform Infrared Spectroscopy (FTIR)

To identify the surface functional groups of the materials, an FTIR with a wavenumber range of 400 to 4000 cm^{-1}

4.4.9 Ultraviolet visible spectroscopy (UV-vis)

The UV absorption of the polymer blends was measured with a UV-vis spectrophotometer (model Cary 5000, manufactured by Varian in the United States) over the wavelength range of 200-800 nm.

4.4.10 Thermoforming test

A manufacturing method that creates a useable product by heating a plastic sheet to a temperature at which it can be molded into a specified shape in a mold and then cutting the sheet to the desired dimensions. The sheet, which is referred to as a film

when referring to thinner gauges and specific types of materials, is placed in an oven and heated to a temperature that is high enough to allow it to be stretched into or onto a mold before it is allowed to cool into its final form. Vacuum forming is an abbreviated form of this process. In the polymer laboratory depicted in Figure 22, a sample was produced through the process of thermoforming.



Figure 22 Thermoforming machine



CHAPTER 5

RESULTS AND DISCUSSION

This chapter describes the results of the morphology, mechanical and thermal properties of PLA/PBS blends and PLA/PBS/EPDM ternary blends. This research was divided into 2 parts. The first part studied PLA and PBS blends ratio at PLA/PBS (90/10), PLA/PBS (80/20), and PLA/PBS (70/30). After that finding the suitable ratio, the second part studied PLA/PBS (80/20) and EPDM ternary blends at the ratio PLA/PBS/EPDM (80/15/5), PLA/PBS/EPDM (80/10/10) and PLA/PBS/EPDM (80/5/15).

5.1 Morphology Properties

5.1.1 PLA/PBS blends

The results of a scanning electron microscope examination into the compatibility of PLA/PBS blends provided an explanation and confirmation of the mechanical property characterization. Figure 23 depicts the phase morphology of the tensile fractured surface of pure PLA and its mixes after a tensile test. The smooth appearance of the pure PLA material's fractured surface, as illustrated in Figure 23(a), is indicative of the material's brittle fracture behavior. Figure 23(b) concurrently indicates that the tensile fracture surface of pure PBS was tensile fractured, exhibiting a more abrasive texture than that of pure PLA, which exhibits ductile behavior.

With the different amounts of PBS, the blends presented different tensile fracture morphologies. Figures 23(c), (d), and (e) show SEM images of PLA/PBS blends with PBS content increasing from 10 to 30 wt%. Figure 23(c) shows SEM image of PLA/PBS (90/10) blends. The addition of PBS increases the roughness of PLA/PBS (90/10) blends. PBS dispersed phase and cavities were generated due to PBS phase detachment during sample fracture. The absence of interactions between PLA and PBS phase. The large distribution in PBS domain size was also observed. This characteristic morphology was also reported in the literature [33]. Figure 23(d) shows SEM image of

PLA/PBS (80/20) blends which display the dispersed PBS phase size increased with increasing PBS contents.

Figure 23(e) shows SEM image of PLA/PBS (70/30) blends which display the larger PBS particles were found on the tensile fracture surface, which is evidence that PBS played a role in promoting phase separation. This was ascribed to the combination of low interfacial adhesion between the PLA and PBS phases and substantially higher viscosity of the PBS dispersed phases in the relatively lower viscosity PLA matrix. Additionally, this was attributed to the low interfacial adhesion between the PLA and PBS phases. In contrast, the fracture surface of blends with 10 and 30 weight percent PBS was smoother, indicating that the material behaved in a brittle manner, and there was good dispersion of PBS throughout the PLA matrix.

However, poor interfacial adhesion between the PLA and PBS phases produced a large number of very small pores, which resulted in a decrease in both the tensile strength and the Young's modulus of the material. This poor adhesion was caused by the thermodynamic incompatibility of the system consisting of PLA and PBS, which resulted in the separation of two phases; as a result, a third component was added. The PLA/PBS (80/20) was selected because its surface at 20 weight percent is rougher than the surfaces of the PLA/PBS (90/10) and the PLA/PBS (70/30).

5.1.2 PLA/PBS/EPDM ternary blends

Figure 24(a) shows the tensile fracture surface of blends of PLA and PBS with a composition of 80/20. As a result of the PBS phase being spread into spherical forms and being implanted in the PLA matrix, the surface of the PLA/PBS blend is rough. This indicated that the PLA and PBS phases were incompatible with one another, or that the phase separation happened as a result of the thermodynamic instability that occurred during the physical blending of the polymers.

Figure 24(b) shows the tensile fractured surface of blends reveals phase separated morphology, which indicates that the EPDM particles are scattered as the spherical form within the PLA matrix. The phase morphology displayed a lack of interfacial adhesion, as evidenced by the surface's presence of empty spherical grooves.

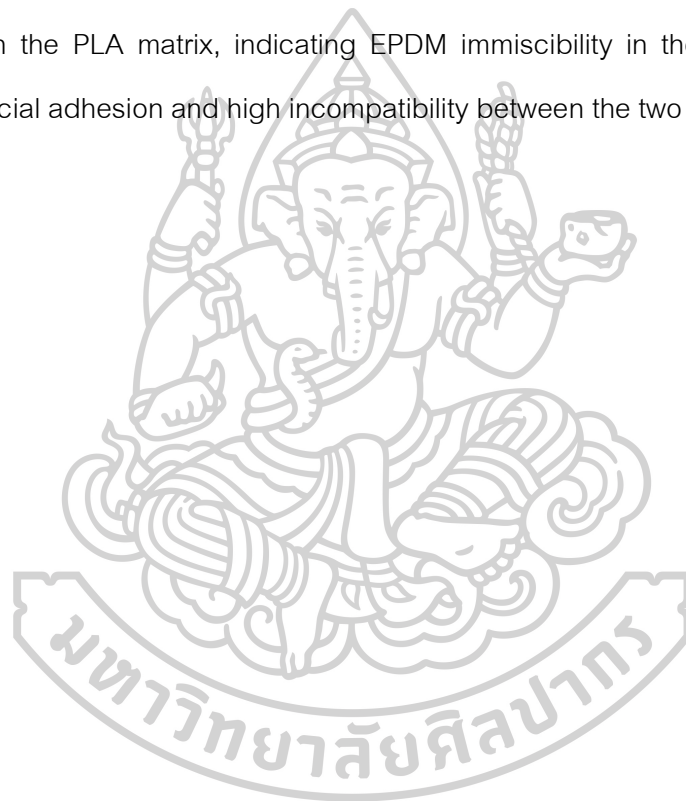
Figure 24(c) shows tensile fracture surface of PLA/PBS/EPDM (80/15/5) ternary blend indicating small crack when the droplet of EPDM is increased with decreasing of EPDM contents. It is observed that the EPDM droplets have some size reduction and homogeneity of the dispersed phase. It is assumed that a slight size reduction of the dispersed phase in the compositions of the studied samples 80/15/5 could be the result of the decreased content of EPDM. The differences in morphology of the studied blends are reflected in the negligible changes of mechanical properties. Moreover, there will be a large number of dispersed fibers. Still, poor fiber distribution in the matrix as a result of high fiber loading leads to the formation of fiber bundles.

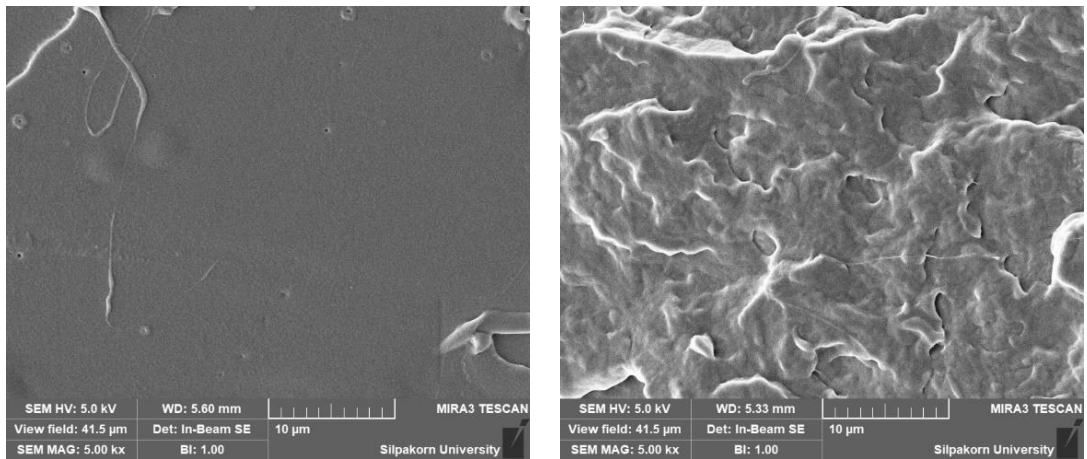
Figure 24(d) shows the tensile fracture surface of PLA/PBS/EPDM (80/10/10) ternary blend tensile fractured surfaces. It can be observed that the size reduction of the PBS fiber is clearly seen. Moreover, a lot of small and large EPDM droplets are dispersed in the PLA matrix which is indicated immiscibility in the PLA matrix due to high incompatibility between the two polymers.

Figure 24(e) shows the tensile fracture surface of PLA/PBS/EPDM (80/5/15) ternary blend tensile fractured surfaces. It can be observed that the dispersion of the biggest EPDM droplets in the PLA matrix phase. As a result of the increased content of EPDM. Moreover, it is observed that the small PBS fiber phase when decreases the content of PBS.

However, the results demonstrated that the addition of PBS did not improve the compatibility of the blends and also altered their mechanical properties. Therefore, the

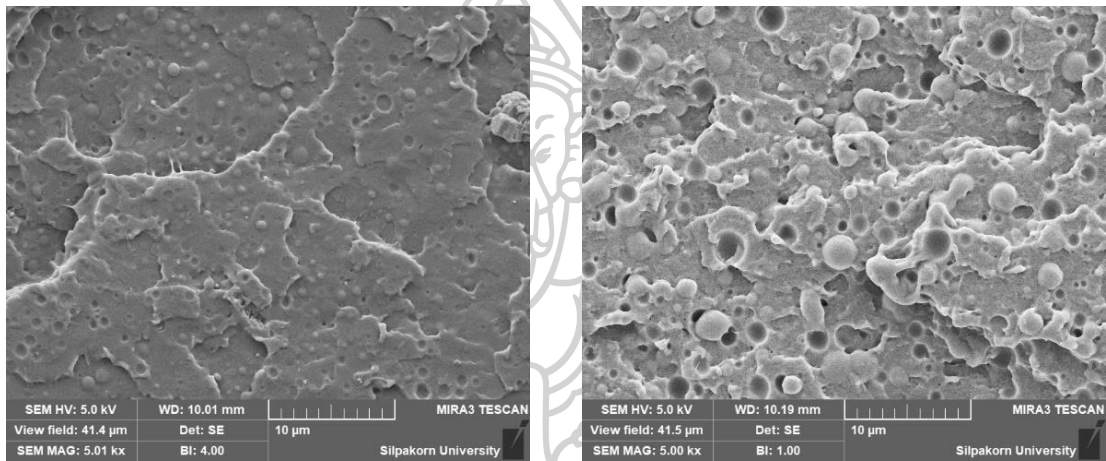
addition of EPDM to the preceding mixture somewhat improves the interfacial adhesion and compatibility of PLA and PBS [34]. Figures 23 and 24 display the SEM micrographs of PLA/PBS blends and PLA/PBS/EPDM ternary blends, respectively. Figure 24 (b-e) illustrates PLA/PBS/EPDM ternary blends and PLA/EPDM blends that were somewhat compatible due to effective EPDM loading, which might marginally improve the compatibility of the aforementioned phases. Clearly observable is the size reduction of the PBS fiber. In addition, a considerable number of small and large EPDM droplets are dispersed in the PLA matrix, indicating EPDM immiscibility in the PLA matrix due to weak interfacial adhesion and high incompatibility between the two polymers [35].





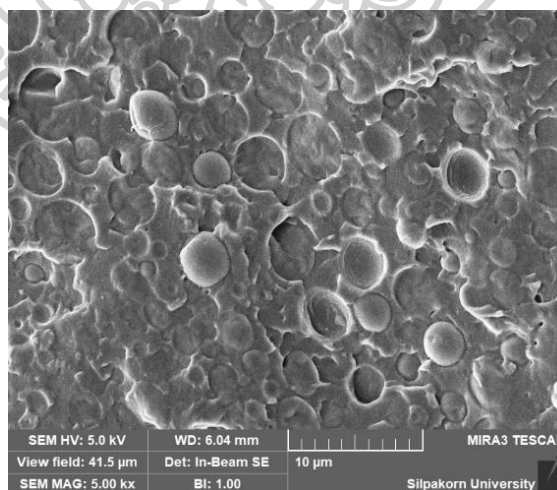
(a) Pure PLA

(b) Pure PBS



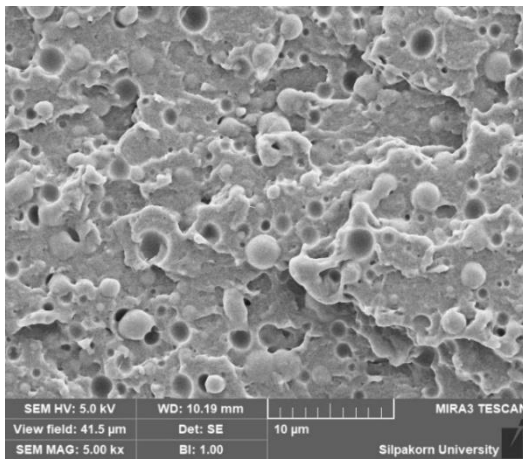
(c) PLA/PBS (90/10)

(d) PLA/PBS (80/20)

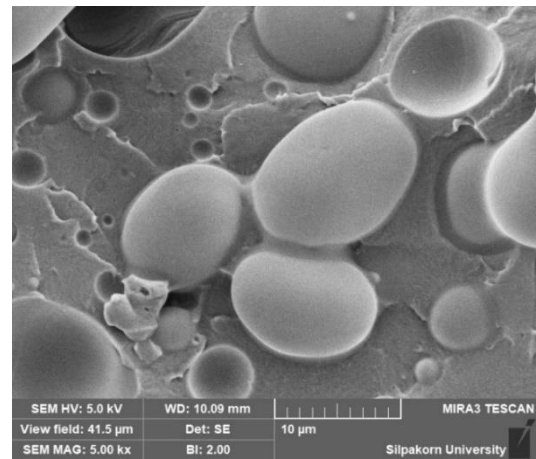


(e) PLA/PBS (70/30)

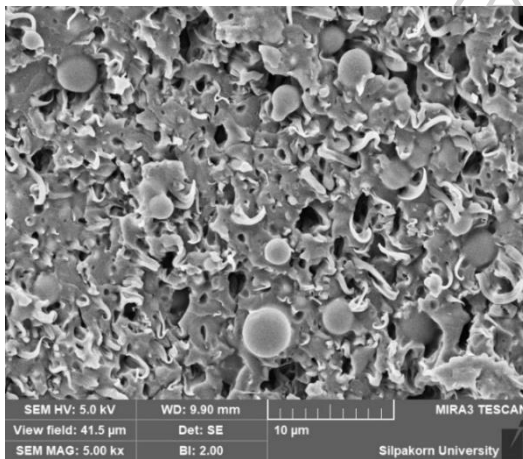
Figure 23 SEM micrographs of the tensile fracture surface of PLA, PBS and PLA/PBS blends at various PBS contents.



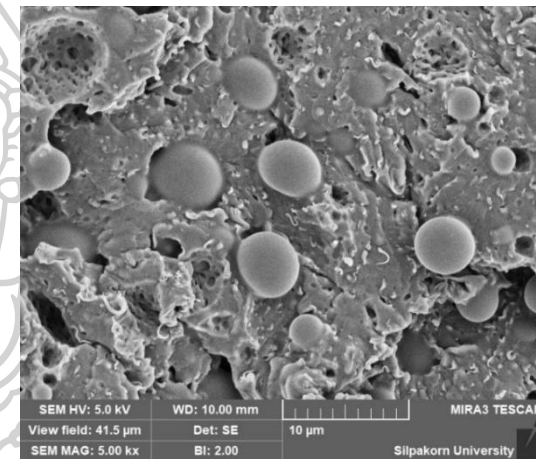
(a) PLA/PBS (80/20)



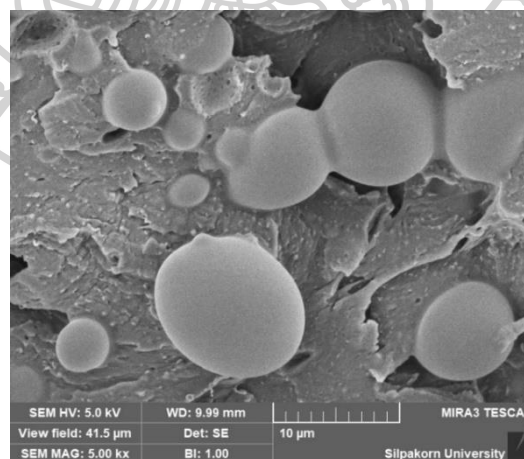
(b) PLA/EPDM (80/20)



(c) PLA/PBS/EPDM (80/15/5)



(d) PLA/PBS/EPDM (80/10/10)



(e) PLA/PBS/EPDM (80/5/15)

Figure 24 micrographs of the tensile fracture surface of PLA/PBS/EPDM ternary blends.

5.2 Mechanical properties

5.2.1 Impact properties

The addition of PBS affects the toughness of the polymer composite and affecting the surface action of PLA and PBS. Figure 25 shows the impact strength of the polymer blends between PLA/PBS tends to increase. Due to the impact behavior of PBS that can resist a lot of impacts. This results in the impact resistance properties of the polymer blend at a ratio of PLA/PBS 80/20 (w/w). Most valuable, However, the addition of large amounts of PBS causes the polymer blend to be more incompatible, making the polymer blend less compatible.

The impact strength of PLA/PBS blends increased with increasing of PBS contents while the impact strength of PLA/PBS/EPDM ternary blends decreased with increasing of EPDM content.

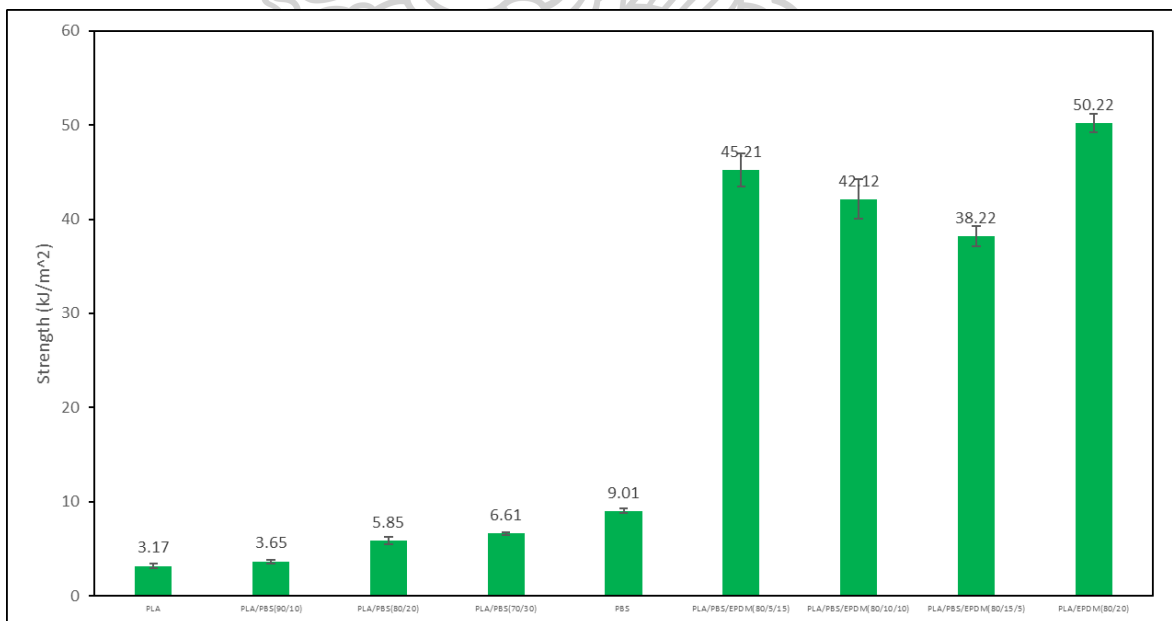


Figure 25 Impact Strength of pure PLA, pure PBS, PLA/PBS blends and PLA/PBS/EPDM ternary blends at different compositions.

5.2.2 Tensile properties

5.2.2.1 PLA/PBS blends

(1) Young's modulus

Figure 26 and Table 3 show Young's modulus of pure PLA, pure PBS, and PLA/PBS blends at different compositions. The results found that Young's modulus of PLA/PBS blends decreased steadily with the addition of PBS. Young's modulus was reduced because Young's modulus of PBS is younger than Young's modulus of PLA.

(2) Tensile strength

Figure 27 and Table 3 show the tensile strength of pure PLA, pure PBS, and PLA/PBS blends at different compositions. The result found that the tensile strength of PLA/PBS blends decreased with increasing PBS contents due to the phase separation as shown in Figure 27, in which morphology showed the poor interaction PLA and PBS phases.

(3) Stress at break

Figure 28 and Table 4 show stress at break of pure PLA, pure PBS, and PLA/PBS blends at different compositions. The result found that stress at break of PLA/PBS blends decreased with increasing PBS content. The results could be confirmed from the dispersed PBS phase size increased when increasing PBS contents, as observed from the SEM micrograph.

(4) Percent strain at break

Figure 29 and Table 4 show the percent strain at break of pure PLA, pure PBS, and PLA/PBS blends at different compositions. The results found that the percent strain at break of PLA/PBS blends decreased with increasing PBS contents. Significantly in 20 wt% of PLA/PBS blends, the percent strain at break massively increased.

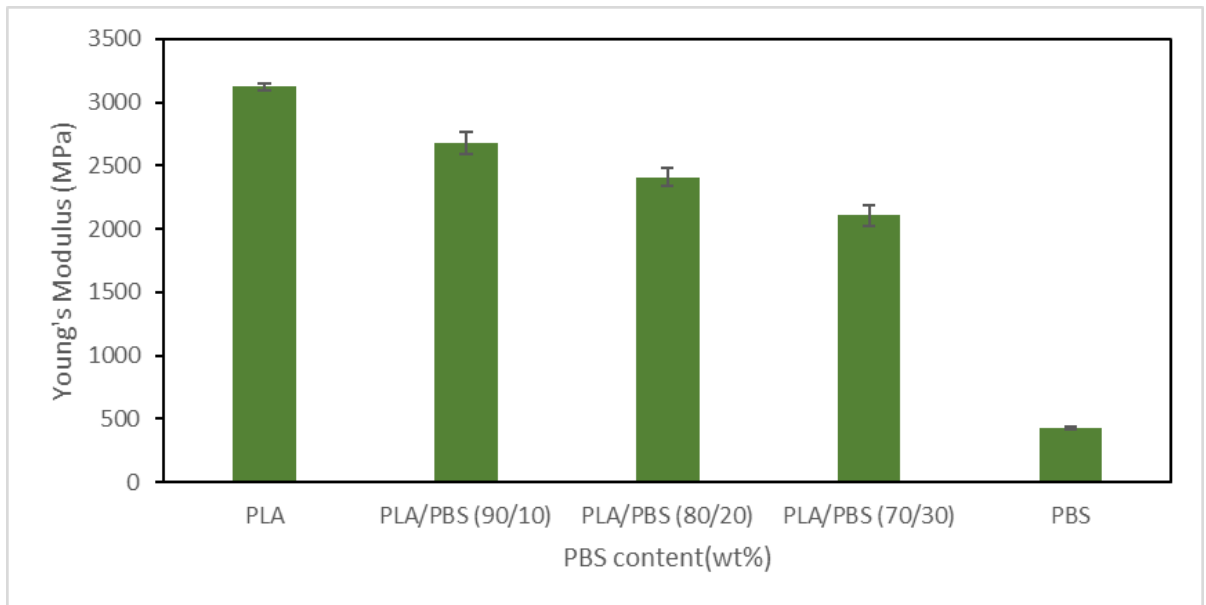


Figure 26 Young's modulus of pure PLA, pure PBS and PLA/PBS blends at different compositions.

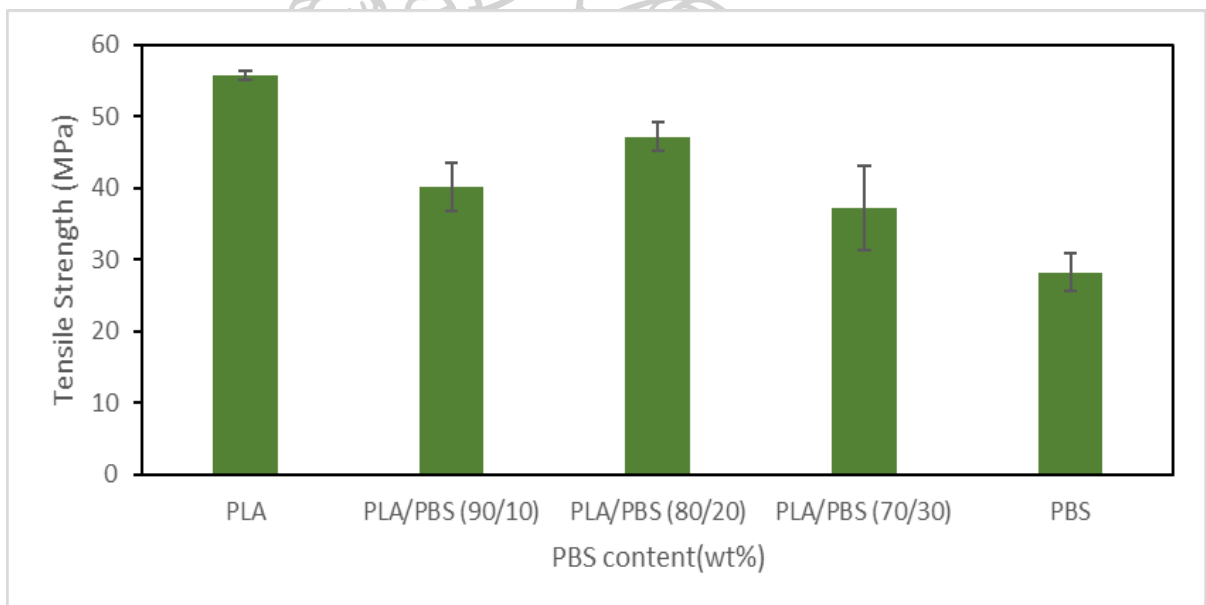


Figure 27 Tensile strength of pure PLA, pure PBS and PLA/PBS blends at different compositions.

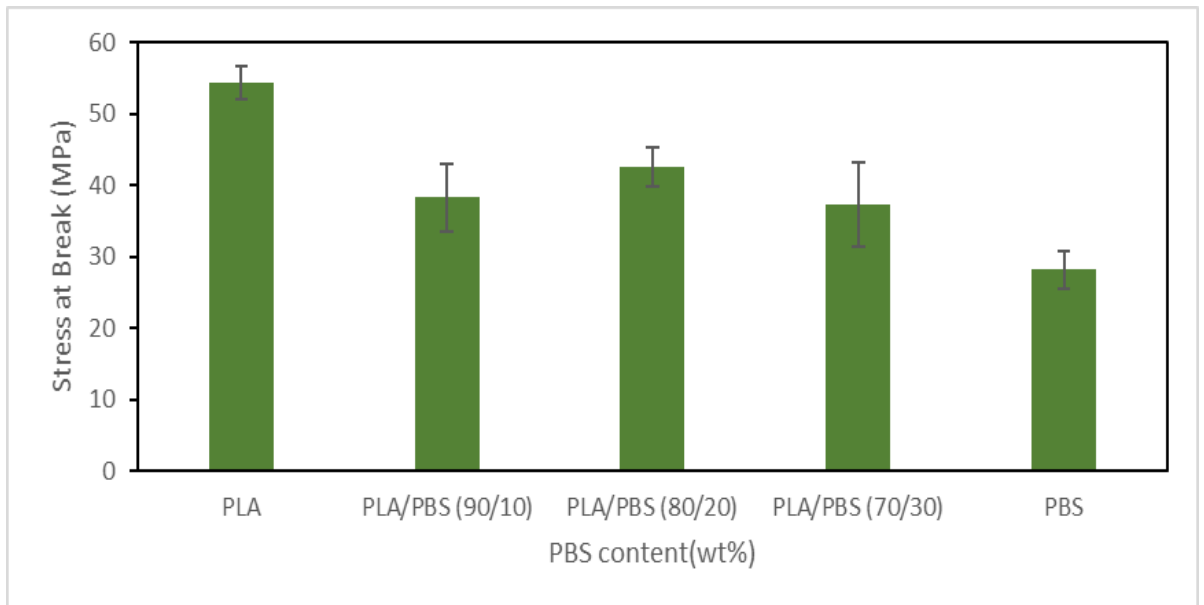


Figure 28 Stress at break of pure PLA, pure PBS and PLA/PBS blends at different compositions.

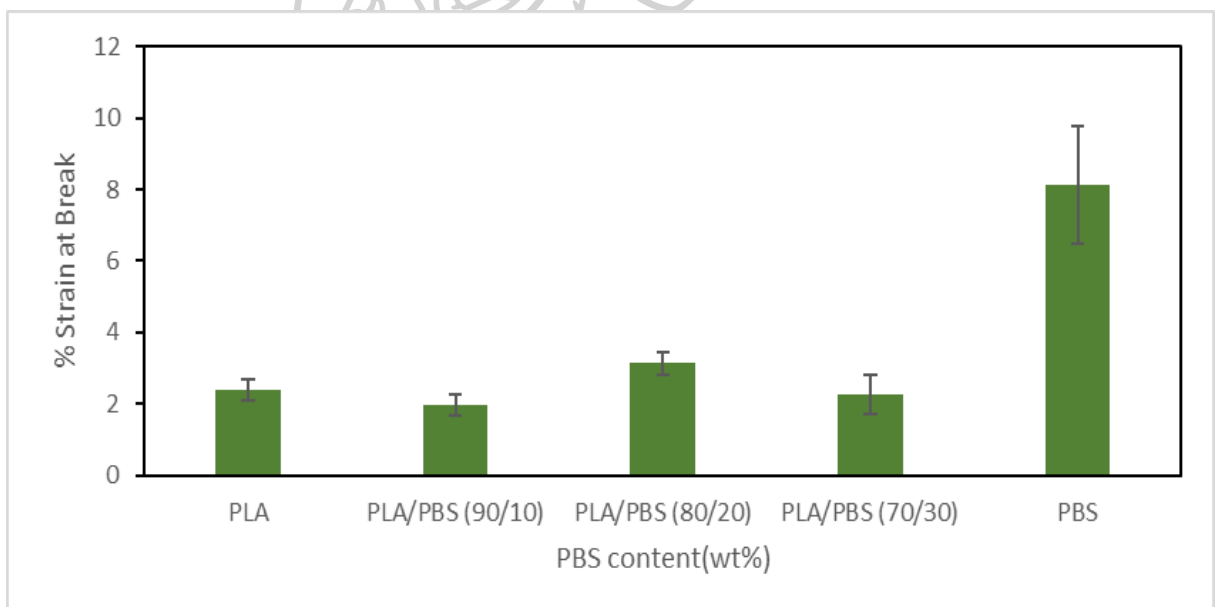


Figure 29 Percent strain at break of pure PLA, pure PBS and PLA/PBS blends at different compositions.

5.2.2.2 PLA/PBS/EPDM ternary blends

(1) Young's modulus

The Young's modulus of PLA/PBS blends mixed with and without EPDM with different ratio are shown in Figure 30. The results showed that the Young's modulus of PLA/PBS blends with differed in the EPDM content. Where various EPDM constituents tended to decrease as EPDM increased, the addition of EPDM to PLA/PBS blends was a combination of results found that the Young's modulus of PLA/PBS/EPDM ternary blends at 80/10/10 and 80/5/15 (w/w) was no different. All constituents showed the reduction due to the morphology of the mixture with EPDM. In this case, EPDM are surface active substances that promote adhesion between the two steps that improve the modulus of young in the PLA/PBS blends mixture.

(2) Tensile strength tensile strength

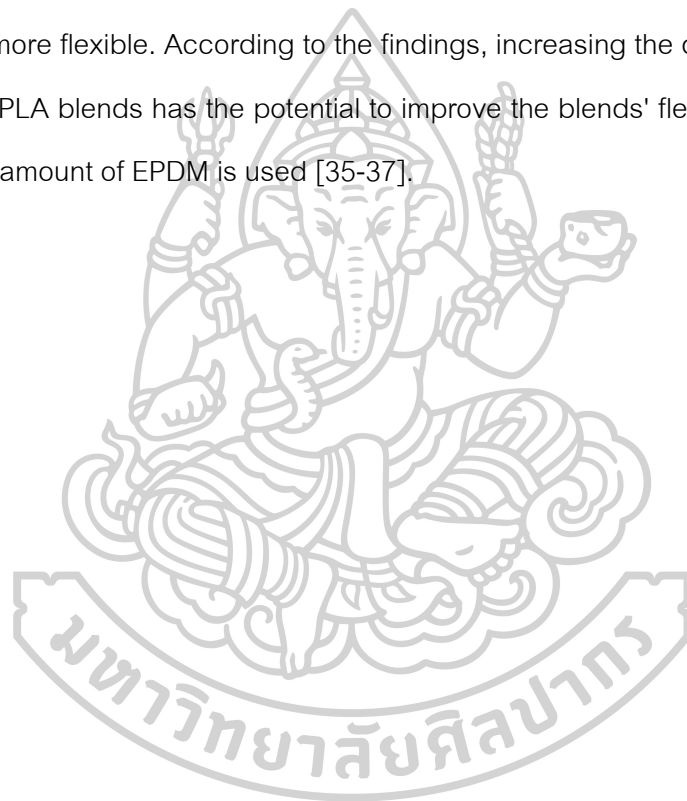
The tensile strength values of PLA/PBAT mixed with and without EPDM with different ratios are shown in Figure 31 and Table3. The Addition of EPDM tends to reduce the tensile strength of polymer blends. However, PLA/PBS/EPDM ternary blend at 80/15/5 (w/w) has an effect on tensile strength due to the morphology. Appeared longitudinal structure and adhesion between PLA and PBS phases are shown in Figure 26

(3) Stress at break

stress at break, stress at break point of the PLA/PBS blended without and with EPDM with different ratio are shown in figure 32, PLA/PBAT break-point stress tends to decrease with addition of EPDM, except for PLA/PBS/EPDM break-point stress 80/5/15. (w/w) was decreased the most.

(4) Percent strain at break

Figure 33 and Table 4, which display the strain at break of PLA/PBS blends, PLA/PBS/EPDM ternary blends, and PLA/EPDM blends, respectively, reveal that the strain at break of PLA/PBS blends with EPDM from 5-20 wt% increased in comparison to PLA pure and PLA/PBS (80/20) blends. When EPDM 20 weight percent was applied, it obviously rose, and this value represents the highest percent strain before breaking. In light of these findings, it is possible to hypothesize that the addition of PBS and EPDM to PLA could improve the % strain at break and toughen the material so that it is more flexible. According to the findings, increasing the quantity of EPDM that is added to PLA blends has the potential to improve the blends' flexibility, but only if the appropriate amount of EPDM is used [35-37].



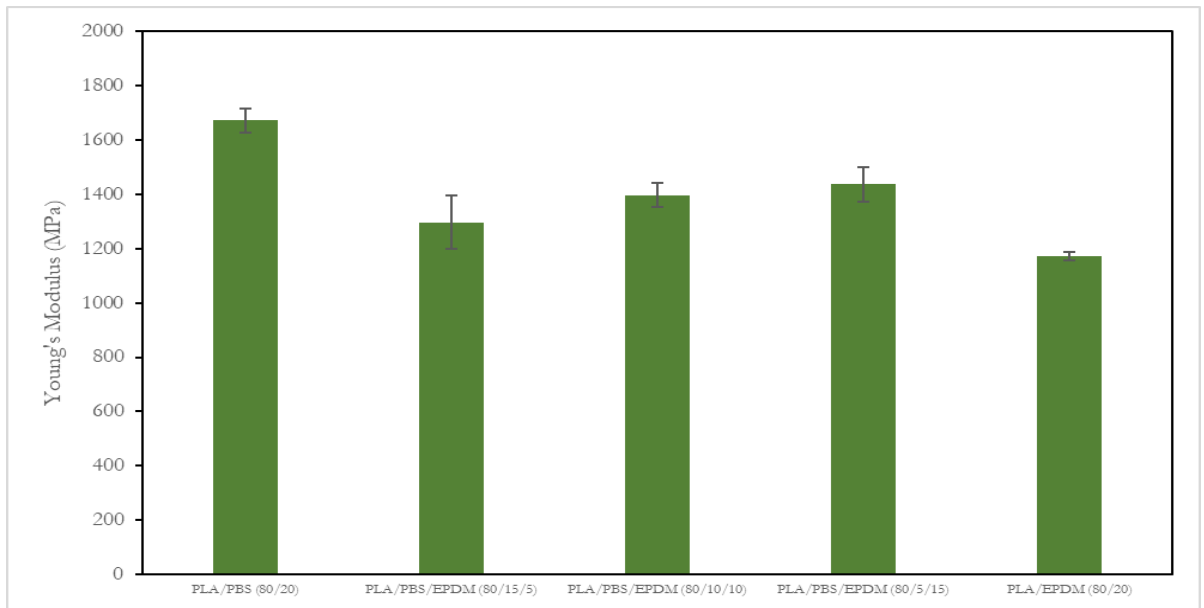


Figure 30 Young's modulus of PLA/PBS/EPDM ternary blends.

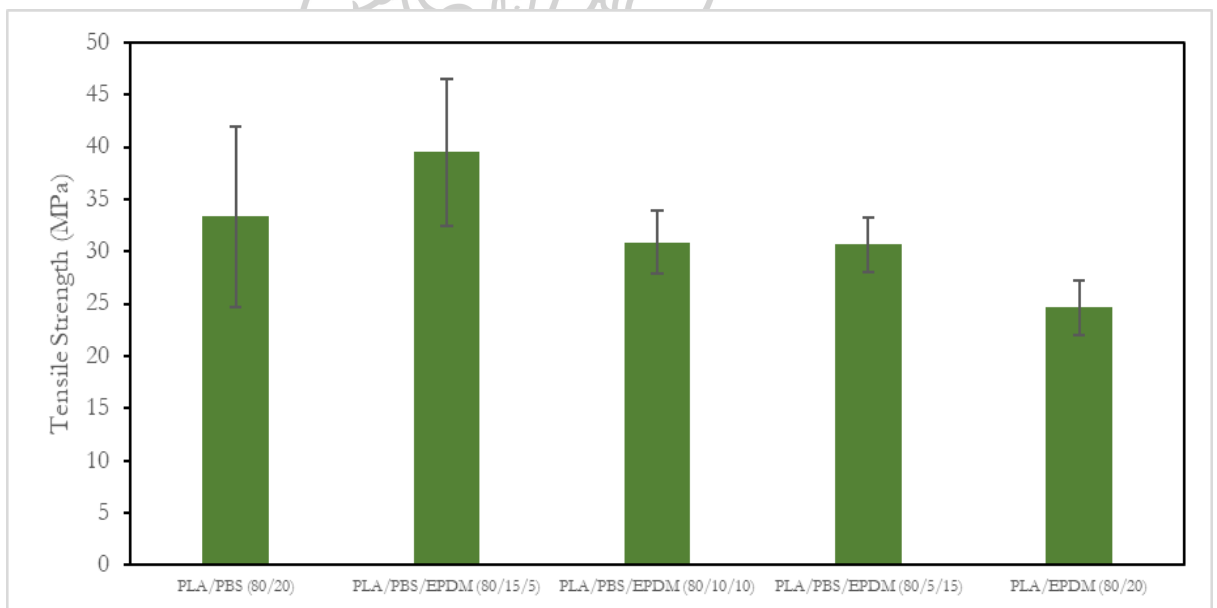


Figure 31 Tensile strength of PLA/PBS/EPDM ternary blends.

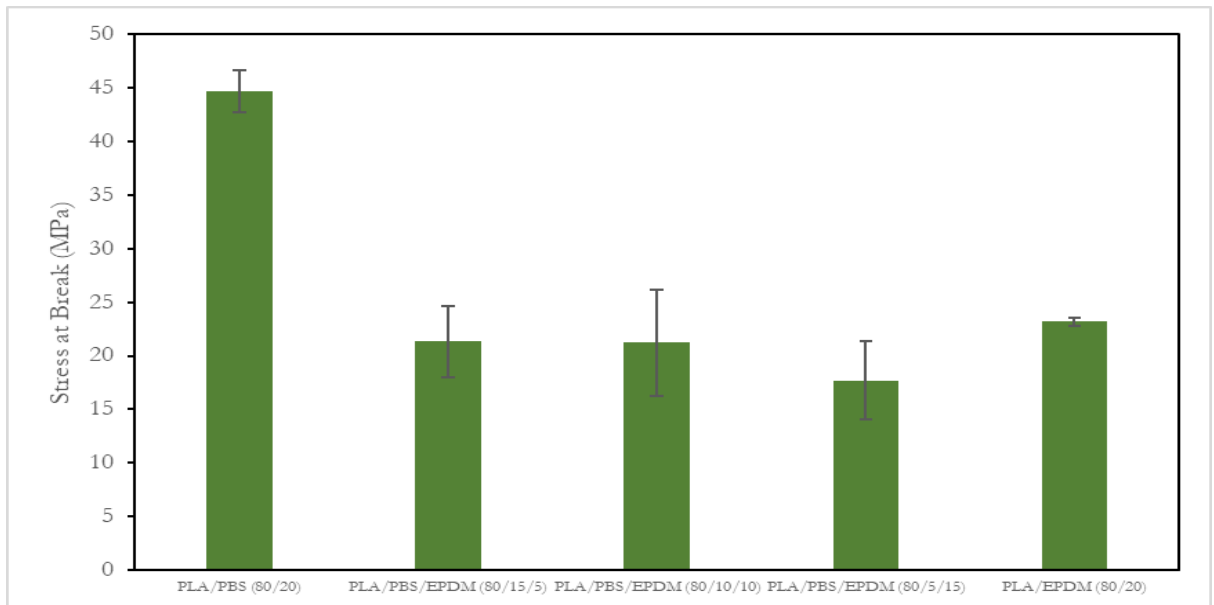


Figure 32 Stress at break of PLA/PBS/EPDM ternary blends.

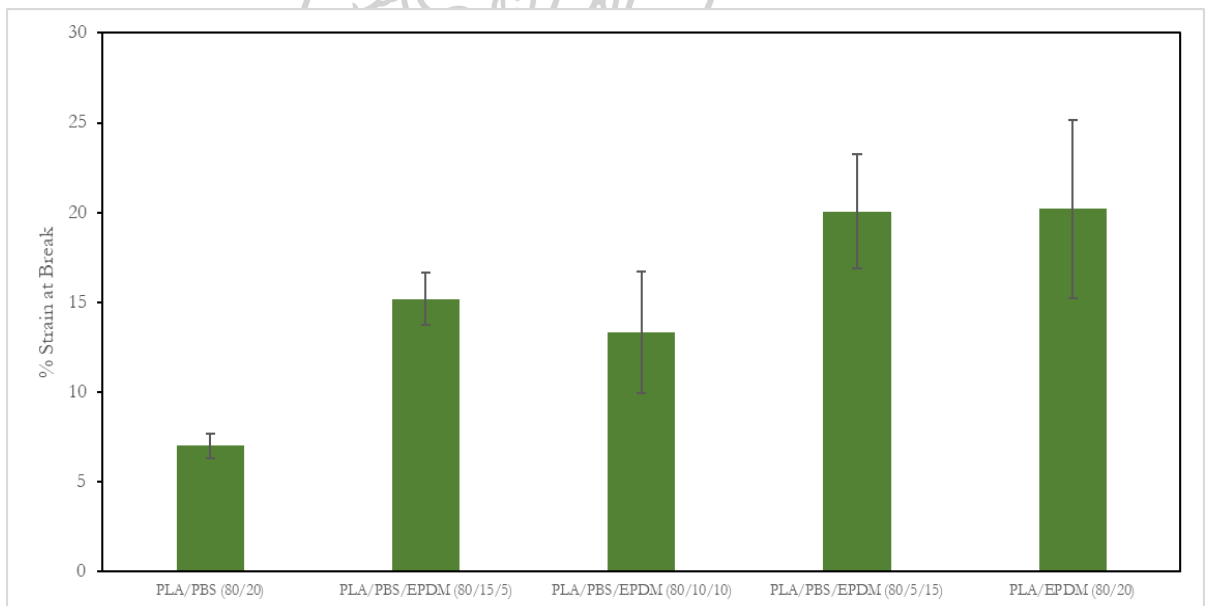


Figure 33 Percent strain at break of PLA/PBS/EPDM ternary blends.

Table 3 Young's modulus and tensile strength of PLA pure, PBS pure, PLA/PBS blends, PLA/PBS/EPDM ternary blends, and PLA/EPDM blends

Sample	Young's modulus (MPa)	tensile strength (MPa)
PLA	3121.89 ± 23.41	55.73±0.68
PBS	422.22±11.68	28.21±2.63
PLA/PBS (90/10)	2676.38±87.21	40.15±3.29
PLA/PBS (80/20)	2410.69±70.54	47.16±2.00
PLA/PBS (70/30)	2106.94±81.39	37.22±5.92
PLA/PBS/EPDM (80/15/5)	1296.87±97.31	39.48±6.98
PLA/PBS/EPDM (80/10/10)	1396.81±45.42	30.86±3.02
PLA/PBS/EPDM (80/5/15)	1436.10±64.26	30.64±2.60
PLA/EPDM (80/20)	1171.69±16.77	24.62±2.61

Table 4 Stress at break and strain at break of PLA pure, PBS pure, PLA/PBS blends, PLA/PBS/EPDM ternary blends, and PLA/EPDM blends

Sample	Stress at break (MPa)	strain at break (%)
PLA	54.28±2.32	2.40±0.28
PBS	28.21±2.63	8.12±1.64
PLA/PBS (90/10)	38.24±4.84	1.96±0.30
PLA/PBS (80/20)	42.54±2.82	3.14±0.31
PLA/PBS (70/30)	37.22±5.92	2.28±0.55
PLA/PBS/EPDM (80/15/5)	21.33±3.33	16.02±1.48
PLA/PBS/EPDM (80/10/10)	21.21±4.97	15.06±3.40
PLA/PBS/EPDM (80/5/15)	17.71±3.68	27.64±3.20
PLA/EPDM (80/20)	23.18±0.37	21.00±4.95

5.3 Thermal properties

5.3.1 DSC analysis

The thermal properties of pure PLA, PLA/PBS blends and PLA/PBS/EPDM ternary blends were investigated from DSC thermograms. DSC is the convenient methods for analyzing the transition such as glass transition temperature, melting and crystallization.

5.3.1.1 The Melting point temperature (T_m)

Melting patterns by the exothermic heating process of pure PLA, PLA/PBS blends and PLA/PBS/EPDM ternary blends were estimated by means of DSC measurements. The melting points temperature (T_m) of pure PLA, PLA/PBS blends and PLA/PBS/EPDM ternary blends are shown in table 5. The melting exothermic showed that PLA had the main melting peak at 149.02 °C. The melting point of PLA/PBS blends was slight decreased when compared with PLA. The results indicated that the crystal structure remained change with the incorporation of compound. And PLA/PBS/EPDM ternary blends the melting temperature was slight decreased when compared with PLA/PBS blends. This result indicated that the incorporation of EPDM had no effect on the melting temperature of blends. The results indicated that the crystal structure remained change with the incorporation of compound.

Table 5 Melting point temperature (T_m) and percentage crystallinity ($\%X_c$) of PLA pure, PBS pure, PLA/PBS, PLA/EPDM blends and PLA/PBS/EPDM ternary blends

Sample	$T_{m,PLA}$ ($^{\circ}C$)	$T_{m,PBS}$ ($^{\circ}C$)	$\%X_{c,PLA}$	$\%X_{c,PBS}$
PLA	149.02	-	25.03	-
PBS	-	116.43	-	50.05
PLA/PBS (90/10)	146.34	112.39	17.28	14.57
PLA/PBS (80/20)	148.08	113.82	12.46	10.51
PLA/PBS (70/30)	148.48	115.34	10.98	9.26
PLA/PBS/EPDM (80/15/5)	147.29	113.70	13.38	11.28
PLA/PBS/EPDM (80/10/10)	148.34	113.87	17.88	15.08
PLA/PBS/EPDM (80/5/15)	148.11	-	18.81	15.87
PLA/EPDM (80/20)	148.21	-	14.01	11.81



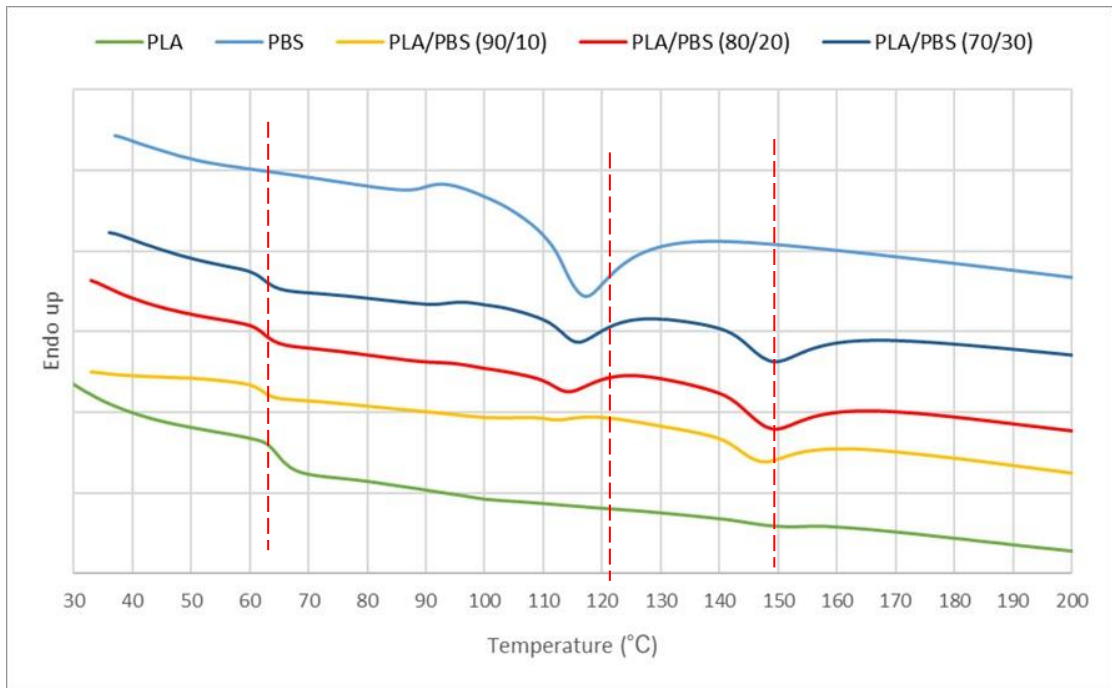


Figure 34 DSC graph of PLA pure, PBS pure, and PLA/PBS blends.

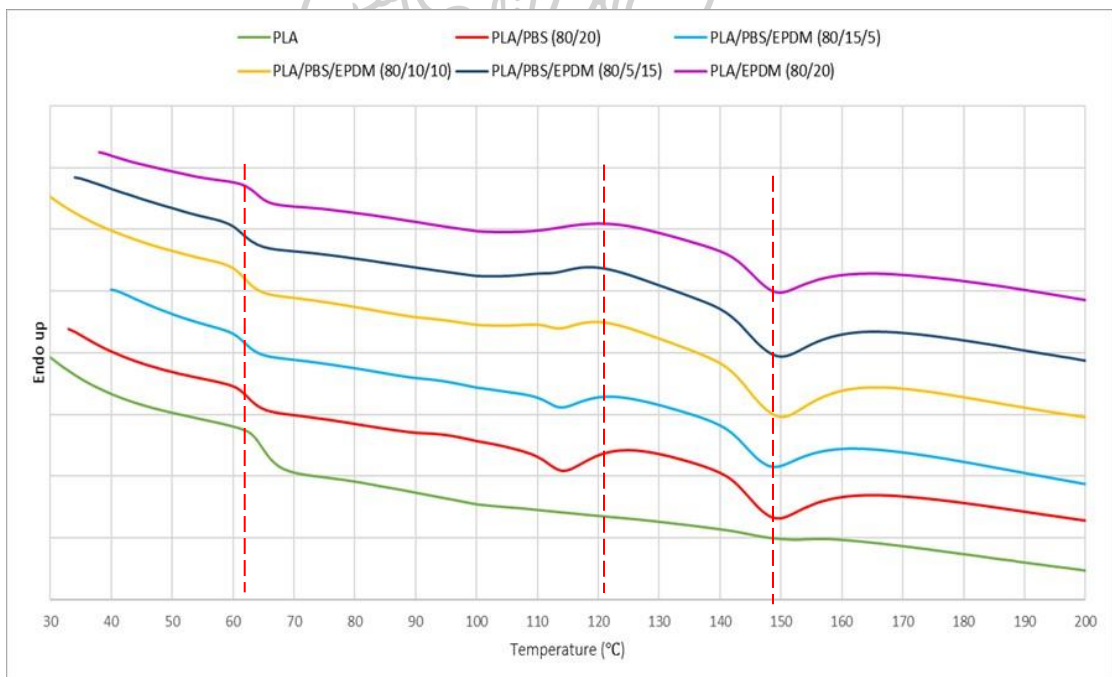


Figure 35 DSC graph of PLA pure, PLA/PBS blends, PLA/EPDM blends, and PLA/PBS/EPDM ternary blends.

5.3.1.2 Percentage crystallinity.

The percentage crystallinity of pure PLA, PLA/PBS blends and PLA/PBS/EPDM ternary blends in table 2. The percentage of crystallinity was calculated based on the following equation:

$$\% \text{Crystallinity} = \frac{\Delta H_c}{\Delta H_m} \times 100 \quad (3)$$

The extrapolated value of the enthalpy related to the melting of a 100% crystalline material is 93.7 J/kg, where ΔH_c is the apparent enthalpy of crystallization. The percentage crystallinity values for pure PLA, blends of PLA and PBS, and ternary blends of PLA, PBS, and EPDM are listed in Table 2 as follows: When the proportion of PBS in the blend was increased, the crystallinity of the PLA/PBS blend decreased. Due to this, it has been discovered that the chain segments have attached themselves to the interface as amorphous PLA chain segments that have entered the crystals. The proportion of PLA and PBS mixtures with crystallinity has grown somewhat. PLA. Crystallinity was discovered to be greater in PLA/PBS/EPDM ternary mixes than in PLA/PBS blends. The percentage of crystallinity in ternary blends of PLA/PBS/EPDM increased somewhat with the addition of EPDM. The percentage of crystallinity was decreased in each of the ternary blends of PLA, PBS, and EPDM compared to pure PLA.

5.3.2 TGA analysis

The thermogravimetric analysis (TGA) was used to investigate the thermal stability of pure PLA, PLA/PBS, and PLA/PBS/EPDM. As a function of temperature, the thermal decomposition of the sample, measured in terms of the percentage of weight loss, was observed and recorded. An index that accurately reflected the heat resistance of the materials was the temperature at which the sample lost one percent of its weight. Table 6 illustrates the decomposition temperatures of 5% weight loss (Td5), 10% weight loss (Td10), and 50% weight loss (Td50) for each blend composition. Td5 refers to the temperature at which a blend composition begins to decompose after 5% of its weight has been lost. When the percentage of PBS in the blend was cut down, an increase in the temperature at which the PLA and PBS compounds decomposed was observable.

Figures 36 show that pure PLA, PLA/PBS blends, and PLA/PBS/EPDM ternary blends all have the same thermogravimetric (TG) curves of dynamic thermal degradation of pure PLA, PLA/PBS, which was observed in the temperature range of 30°C to 600°C at heating rates of 10°C/min. These results can be found by comparing the two sets of figures. When looking at pure PLA, PLA/PBS, it is clear that the thermal degradation of pure PLA progresses by one degradation step found that decomposition beginning at approximately 300 °C. The beginning degradation temperature of the blends tended to increase in a parabolic fashion as the proportion of PBS in the mixture increased. The breakdown of EPDM can be seen to occur at temperatures ranging from 360 to 460 °C.

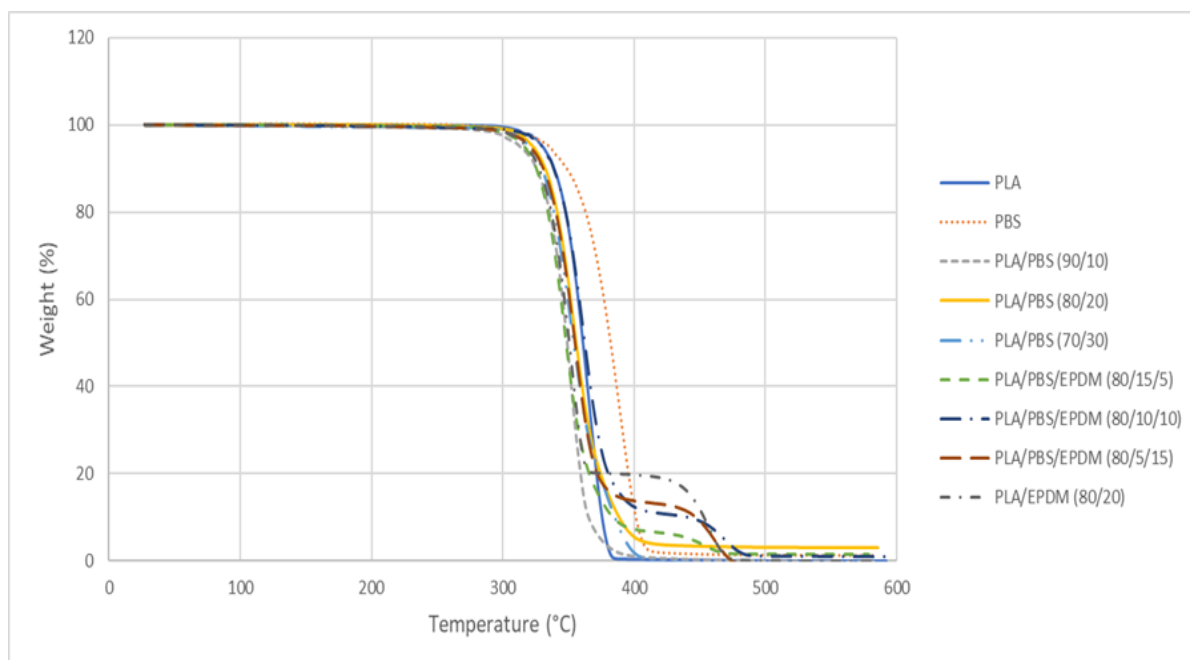


Figure 36 TGA thermograms of PLA PLA/PBS and PLA/PBS/EPDM blends.

Table 6 Decomposition temperature of PLA, PLA/PBS and PLA/PBS/EPDM.

Samples	Temperature (°C)		
	T_{d5}	T_{d10}	T_{d50}
PLA	330.12	338.80	360.94
PBS	345.40	358.41	391.84
PLA/PBS (90/10)	319.18	331.47	355.09
PLA/PBS (80/20)	328.95	338.34	361.97
PLA/PBS (70/30)	328.74	338.58	362.76
PLA/PBS/EPDM (80/15/5)	329.31	338.47	361.17
PLA/PBS/EPDM (80/10/10)	328.80	337.48	361.33
PLA/PBS/EPDM (80/5/15)	327.27	337.56	361.83
PLA/EPDM (80/20)	329.03	338.53	361.56

5.4 Thermomechanical Properties

5.4.1 PLA/PBS blends

The thermomechanical properties of pure PLA and PLA/PBS blends as examined by DMA. The variation of storage modulus of the blends is shown in Figures 37. The storage modulus decreased when the temperature increased (50 °C – 60 °C). After temperature at 65 °C storage modulus was sharply decreased to a glass transition temperature and constant at temperature range 70 °C – 90 °C (rubber state) about 100 MPa and highest increased to 700 MPa at 110 °C

The storage modulus of PLA/PBS blends trend to decrease when the temperature increased (50°C - 60°C). After temperature at 65 °C storage modulus sharply decreased to glass transition and at temperature range 70 °C – 90 °C (rubber state) about 100 MPa and highest increased to 710 MPa at 110 °C at PLA/PBS (80/20). The increase of storages modulus refers to the cold crystallization of the amorphous PLA when increased PBS content.

5.4.2 PLA/PBS/EPDM ternary blends

The storage modulus of pure PLA and PLA/PBS/EPDM ternary blends with was examined by DMA. Figures 38 shown the variation of storage modulus of the pure PLA, PLA/PBS/EPDM (80/15/5), PLA/PBS/EPDM (80/10/10), PLA/PBS/EPDM (80/5/15) and PLA/EPDM (80/20) blend. The storage modulus decreased when the temperature increased (40°C - 55°C). After temperature at 55°C storage modulus was sharply decreased to a glass transition temperature and constant at temperature range 65°C – 90°C (rubbery state) about 90 MPa and highest increased to 900 MPa at 110°C at PLA/PBS/EPDM (80/15/5). The increase of storage modulus refers to the cold crystallization of the amorphous PLA when increased PBS and EPDM content.

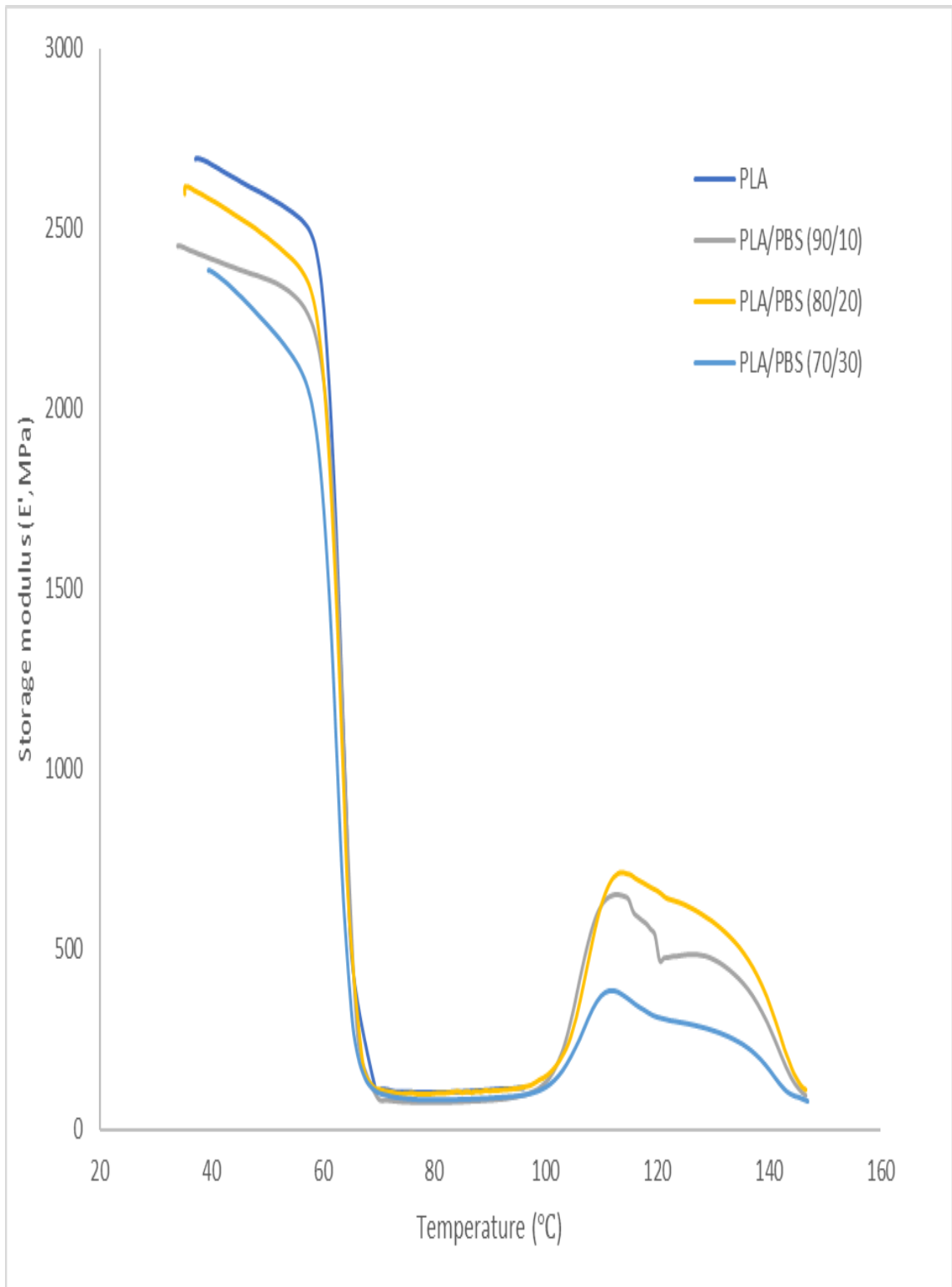


Figure 37 Storage modulus of pure PLA and PLA/PBS blends with PBS contents.

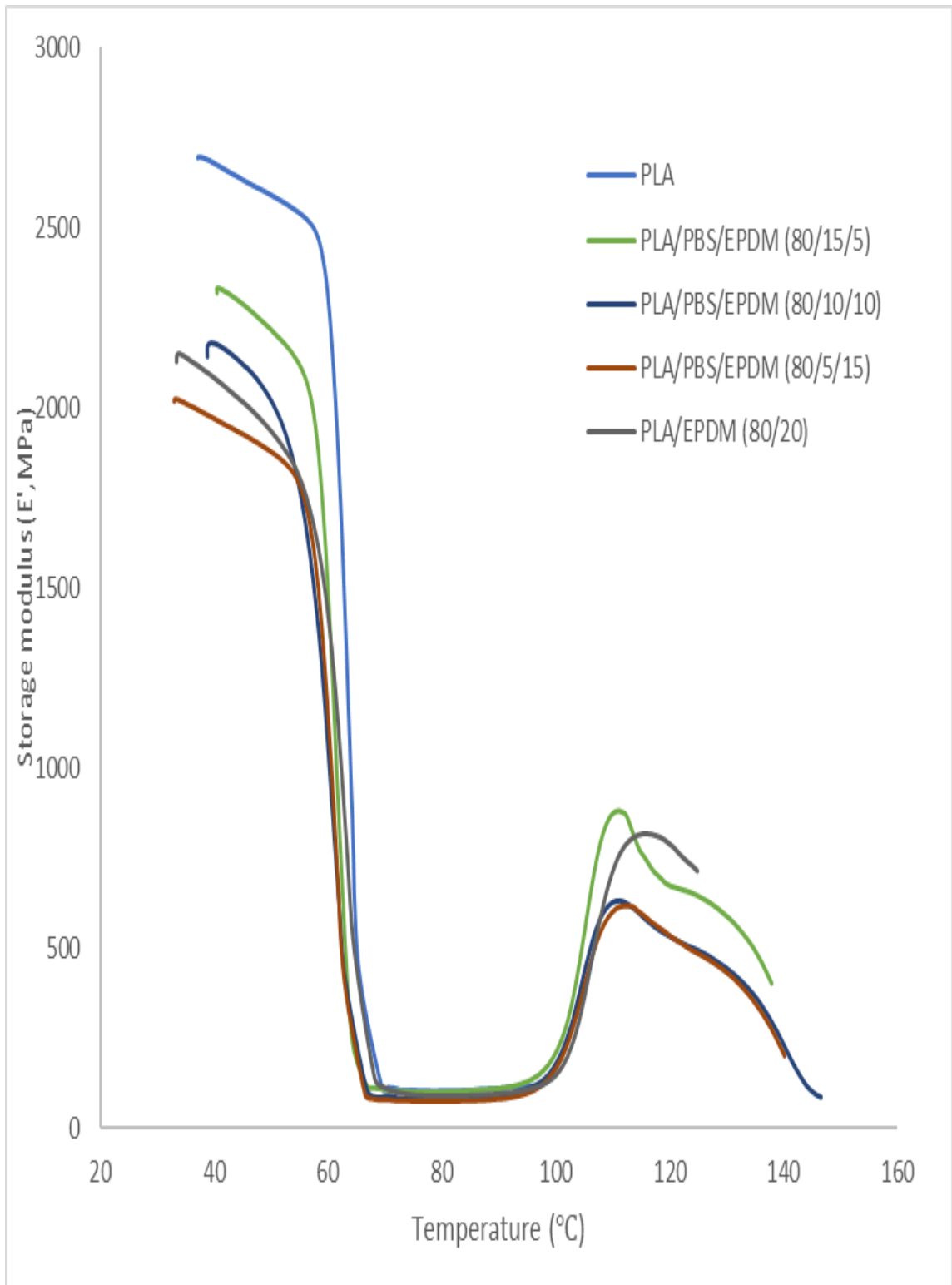


Figure 38 Storage modulus of pure PLA and PLA/PBS/EPDM ternary blends with EPDM contents

5.5. XRD analysis

The XRD analysis was used to obtain further insight into the materials crystallinity of material. Figure 39 shows the XRD patterns of pure PLA, pure PBS and pure EPDM which display the XRD patterns of PLA a broad diffraction peak centered at $2\theta \approx 16^\circ$. The PLA did not show any characteristic peak which indicates that the structure is amorphous. This corresponds to the characteristic peak of PLA [38, 39] and indicates the development of a certain crystallinity degree after blending. The XRD patterns of PBS shows the peak at $2\theta \approx 19.21^\circ$, 21.45° and 25.79° due to its crystalline of PBS[40]. The XRD patterns of EPDM shows a broadening small peak at $2\theta \approx 18^\circ - 20^\circ$ indicates that the structure is amorphous[41].

Table 7 displays the normalized peak area for ease of reference. According to the findings, the crystallinity had somewhat risen as a result of the crystalline PBS, which exhibited as peaks of crystallinity in the XRD patterns displayed in Figure 40. This was due to the fact that PBS is crystalline. Figure 41 displays the XRD patterns that were produced by the ternary blend. However, the patterns of PLA/PBS/EPDM (80/15/5) ternary blends demonstrate the presence of semi-crystalline areas at $2\theta \approx 22.27^\circ$. Peaks indicative of amorphous structure were observed in the XRD patterns of both PLA/PBS/EPMD (80/10/10) and PLA/PBS/EPMD (80/5/15). This suggested that the amount of EPDM might change both the crystalline structure and the composition of the PLA/PBS blends, as shown in Table 5. This was in line with the findings of the DSC, which demonstrated a modest drop in the melting temperature of PLA blends when a high quantity of EPDM and PBS was added.

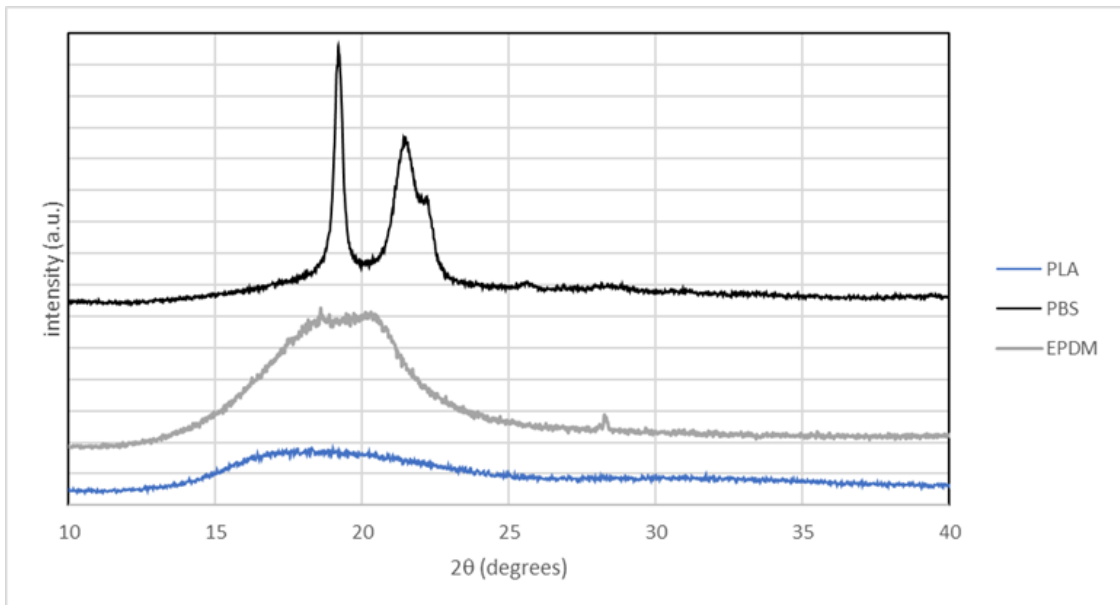


Figure 39 The XRD patterns of pure PLA, pure PBS and pure EPDM.

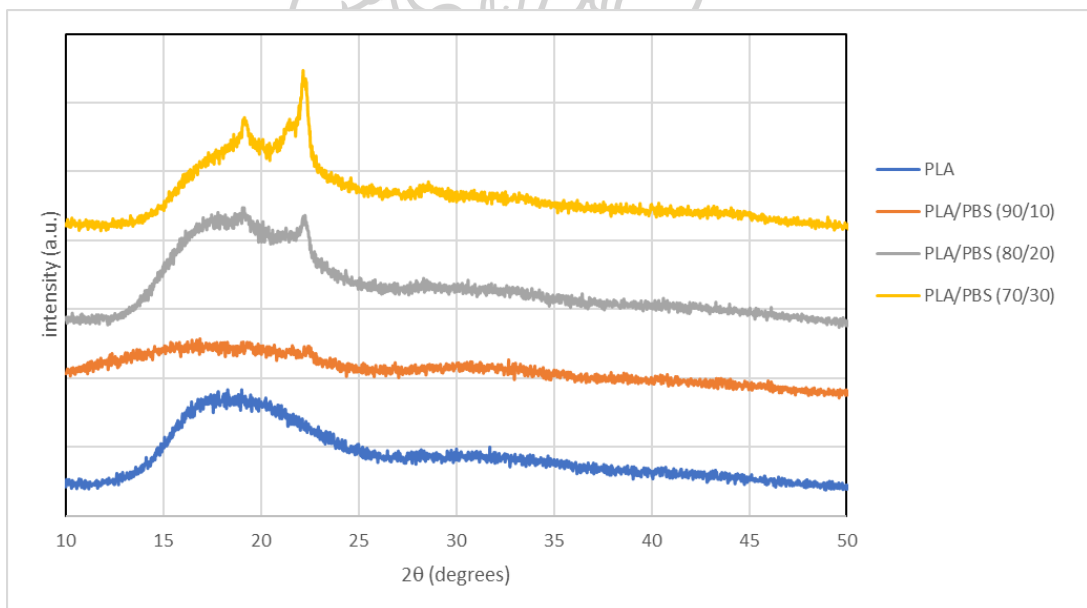


Figure 40 The XRD patterns of pure PLA, and PLA/PBS blends with various weight ratios.

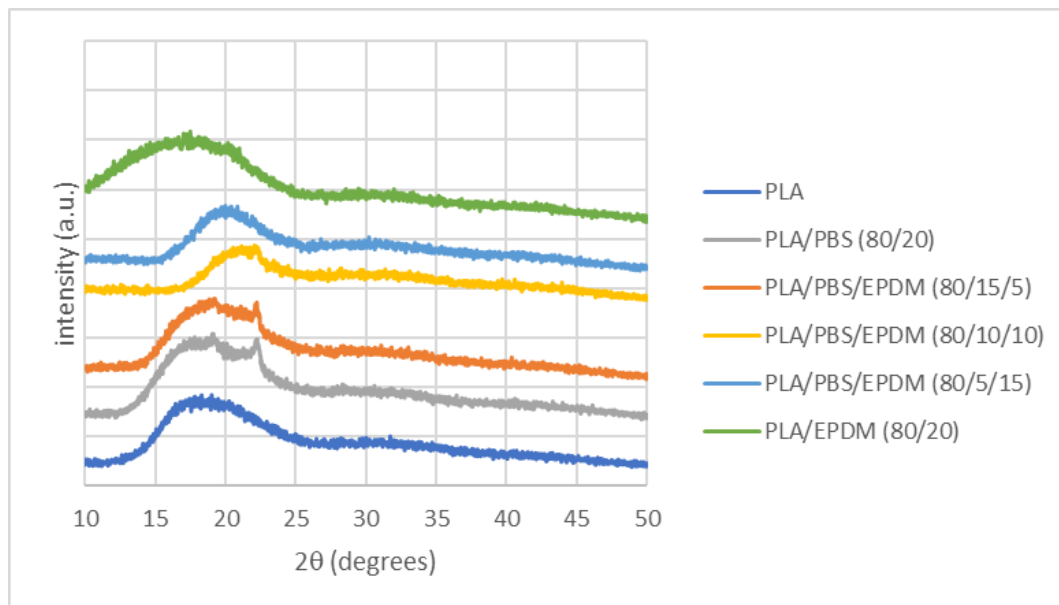


Figure 41 The XRD patterns of pure PLA, and PLA/PBS/EPDM ternary blends with various weight ratios.

Table 7 Normalized crystallinity of blends and ternary blends.

Sample	Area		Xc (%)
	Crystalline	Amorphous	
PLA	-	1809.08	16.92
PBS	3623.47	-	38.39
EPDM	-	5649.67	44.32
PLA/PBS (90/10)	-	1307.48	2.27
PLA/PBS (80/20)	2897.28	2960.15	49.46
PLA/PBS (70/30)	454.88	1836.42	19.85
PLA/PBS/EPDM (80/15/5)	93.41	1324.19	6.59
PLA/PBS/EPDM (80/10/10)	-	1245.32	49.77
PLA/PBS/EPDM (80/5/15)	-	1115.85	59.90
PLA/EPDM (80/20)	-	1371.60	68.13

5.6. FTIR analysis

The FTIR was utilized to determine the surface chemistry of PLA/PBS, PLA/EPDM, and PLA/PBS/EPDM ternary blends based on changes in the vibration modes and band position between 400 and 4000 cm^{-1} . Figure 42 depicts the FTIR spectra of PLA pure, PLA/PBS (80/20), PLA/EPDM (80/20), and PLA/PBS/EPDM ternary blends with varying ratios. The spectra of the PLA sample revealed four distinct absorption bands centered at 1,750 cm^{-1} (C=O stretching vibration), 2,945 cm^{-1} and 2,995 cm^{-1} (C-H aliphatic stretching), and 3,510 cm^{-1} corresponding to the motions of O-H stretching vibrations[42]. The typical carbonyl peak at 1,750 cm^{-1} was moved to 1,716 cm^{-1} when the PBS concentration in PLA was increased to 20% by weight. This result suggests that PLA and PBS were partially miscible. Figure 23 illustrates the interaction between the C=O, C-O, and -OH at the end of the molecular chain of both PLA and PBS, in accordance with the morphological analysis results.

The three peaks between 1100 and 1350 cm^{-1} in the FTIR spectrum of EPDM are ascribed to C-H stretching bands. The peaks between 1570 and 1850 cm^{-1} correspond to C-H stretching bands. And the third one, which has C-H combination bands with significantly higher absorptivity than the bands in regions one and two and is positioned between 1950 and 2500 cm^{-1} [43, 44]. The carbonyl group (C=O) of PLA remained unchanged, indicating that there were no interactions between PLA and EPDM. The FTIR spectra of ternary blends of PLA/PBS/EPDM were identical. Because there were no modifications, it confirmed that the PLA and EPDM mixtures are not miscible.

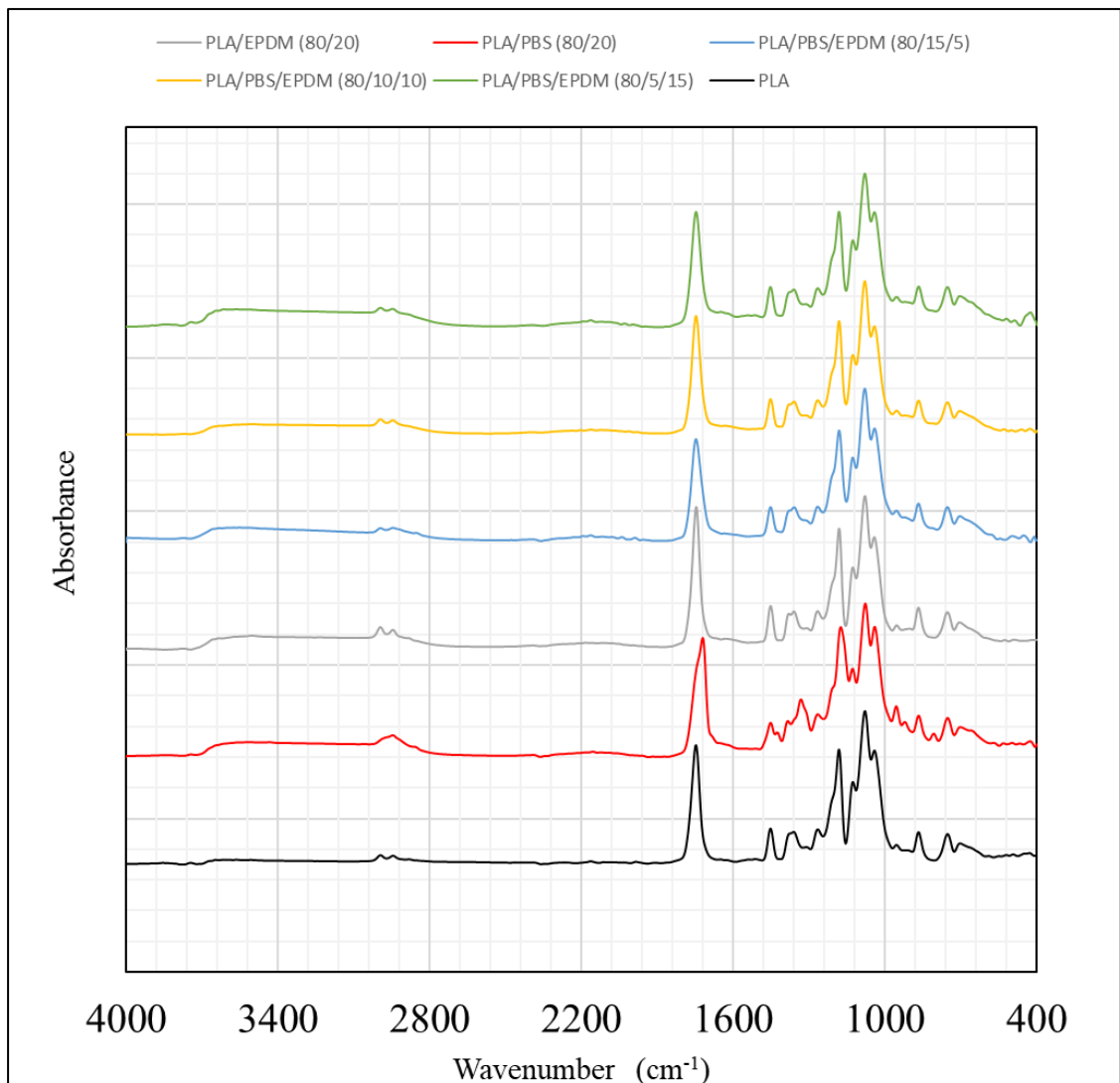
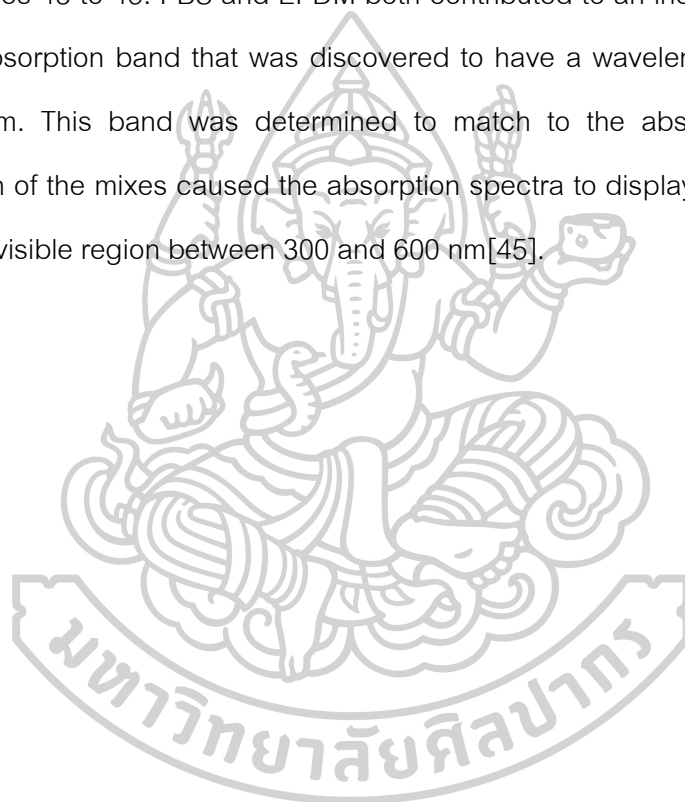


Figure 42 FTIR spectra of PLA pure, PLA/PBS (80/20), PLA/EPDM (80/20) and PLA/PBS/EPDM ternary blends with various ratio.

5.7. UV- vis analysis

The UV-vis spectrophotometer was used to analyze the UV absorption of PLA, PLA/PBS blends, and PLA/PBS/EPDM ternary mixes in the 200-600 nm wavelength range. There are two distinct ranges that make up UV absorption: the UV region and the visible region. The ultraviolet (UV) absorbance of the mixes and ternary mixtures can be seen in figures 43 to 45. PBS and EPDM both contributed to an increase in the intensity of a high absorption band that was discovered to have a wavelength that was shorter than 230 nm. This band was determined to match to the absorption of PLA. The discoloration of the mixes caused the absorption spectra to display a strong absorption band in the visible region between 300 and 600 nm[45].



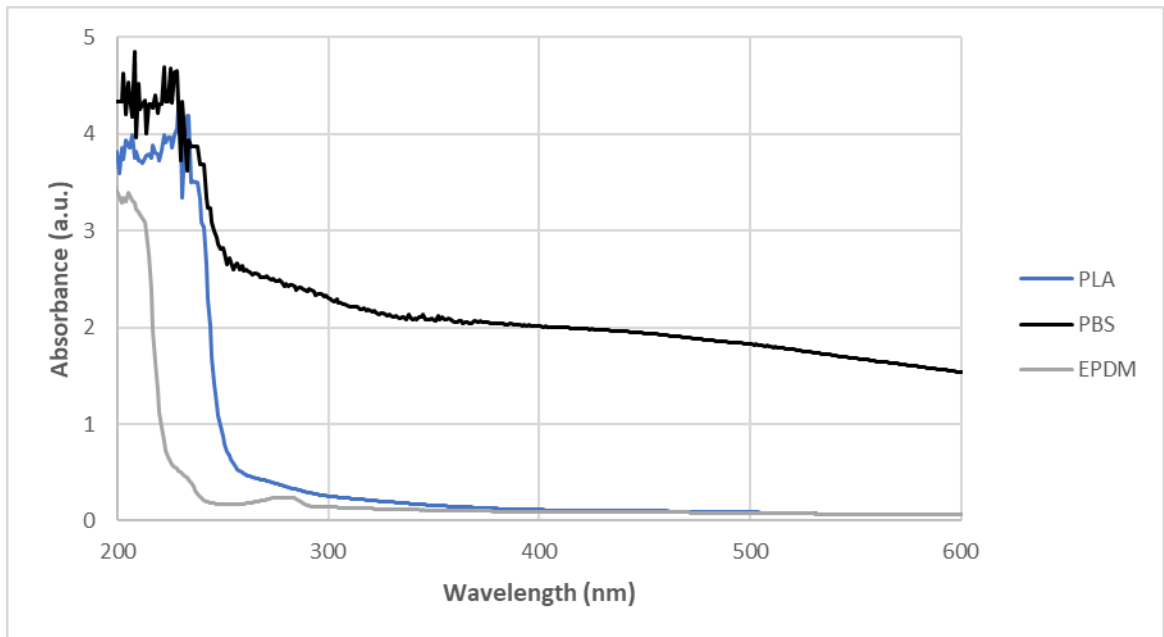


Figure 43 UV-vis of PLA, PBS and EPDM.

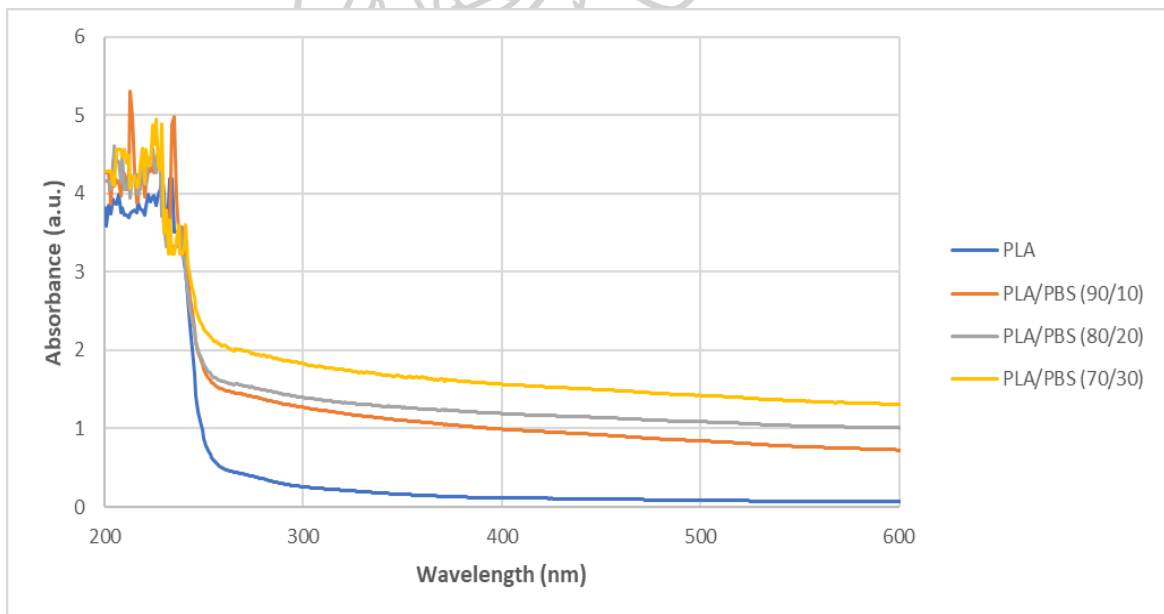


Figure 44 UV-vis of PLA and PLA/PBS blend various contents.

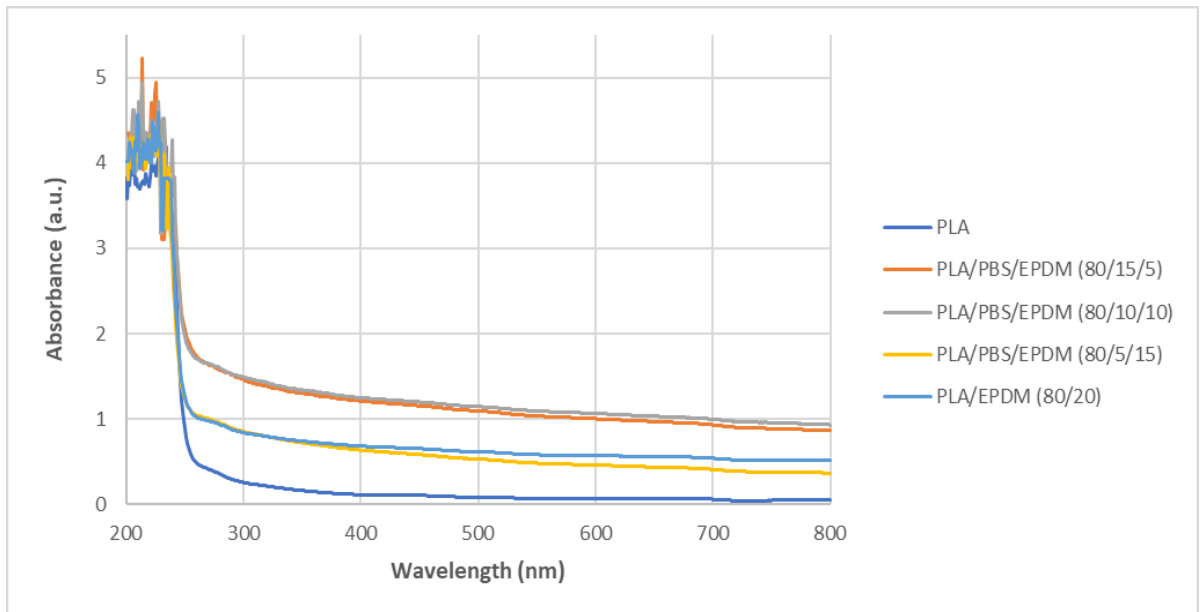
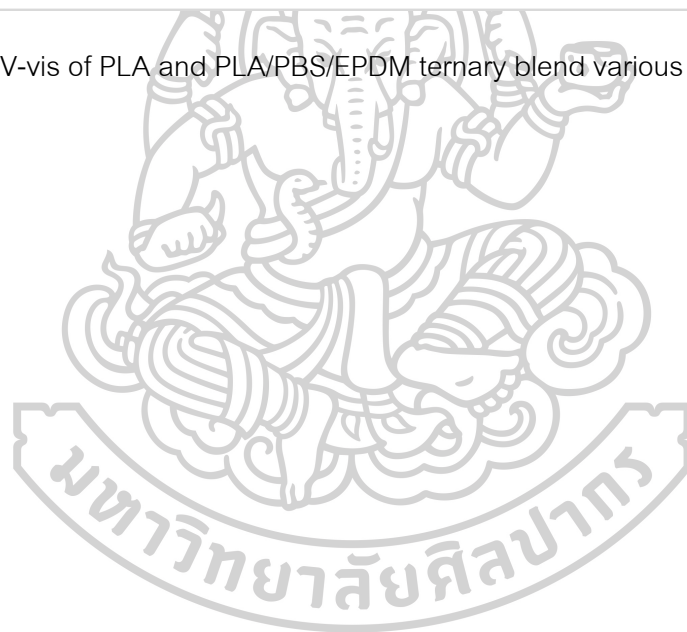


Figure 45 UV-vis of PLA and PLA/PBS/EPDM ternary blend various contents.



5.8. Packaging from thermoforming

The thermoforming machine is used to create a simple workpiece such as bottle, plastic bag, bowl. The mold for thermoforming is also simple small glass or bottle cap. The thermoforming process is thermal forming process after sample is heated more than softening point. Then the sample is extended into product. The neat PLA is brittle, transparent and thin. Consequently, the neat PLA is not suitable for thermoforming as show in Figure 46.

5.8.1 PLA/PBS blends

The PLA/PBS blends can be formed with thermoforming into packaging product better than neat PLA. However, it's still thin and brittle. In this section, the different ratio of PLA/PBS (90/10), PLA/PBS (80/20) and PLA/PBS (70/30) blends were also evaluated as showed in Figure 47-49.

5.8.2 PLA/PBS/EPDM ternary blends

The PLA/PBS (80/20) was selected to blend with EPDM as ternary blends which it can be form easily compared to PLA/PBS blends. The addition of EPDM increased toughness of PLA/PBS blends as showed in Figure 50-52.

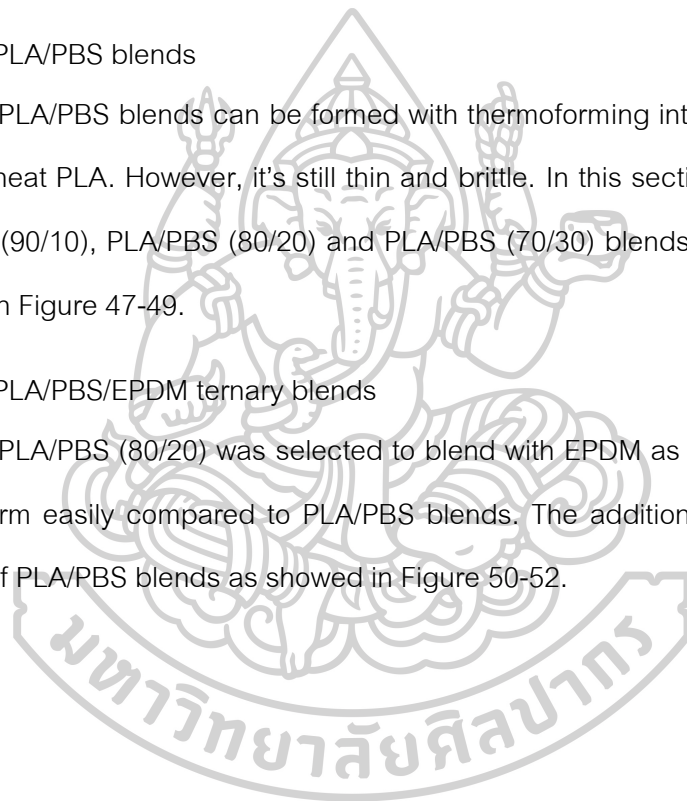




Figure 46 Neat PLA packaging from thermoforming

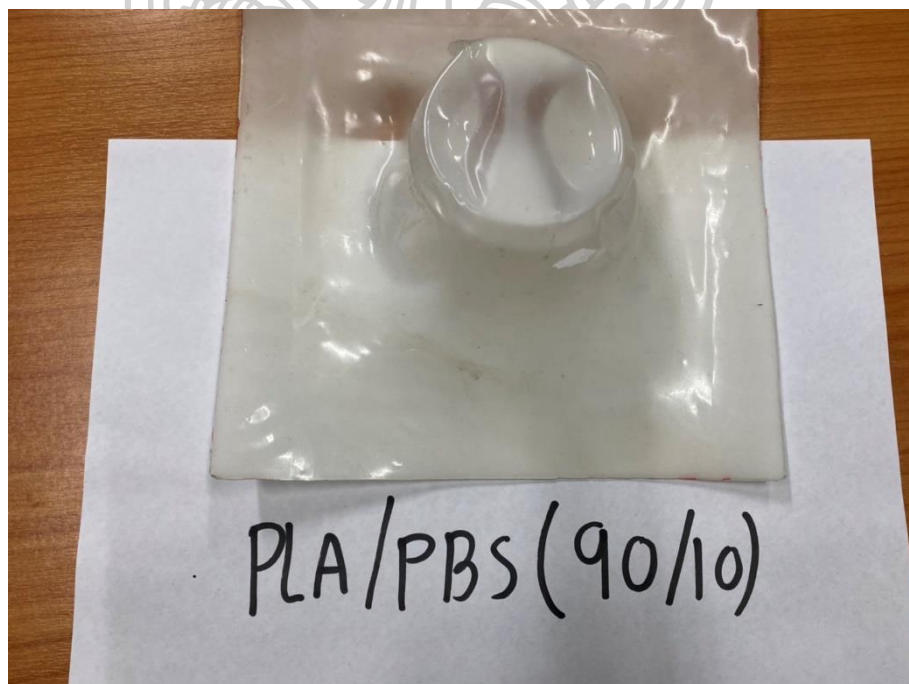


Figure 47 PLA/PBS (90/10) packaging from thermoforming

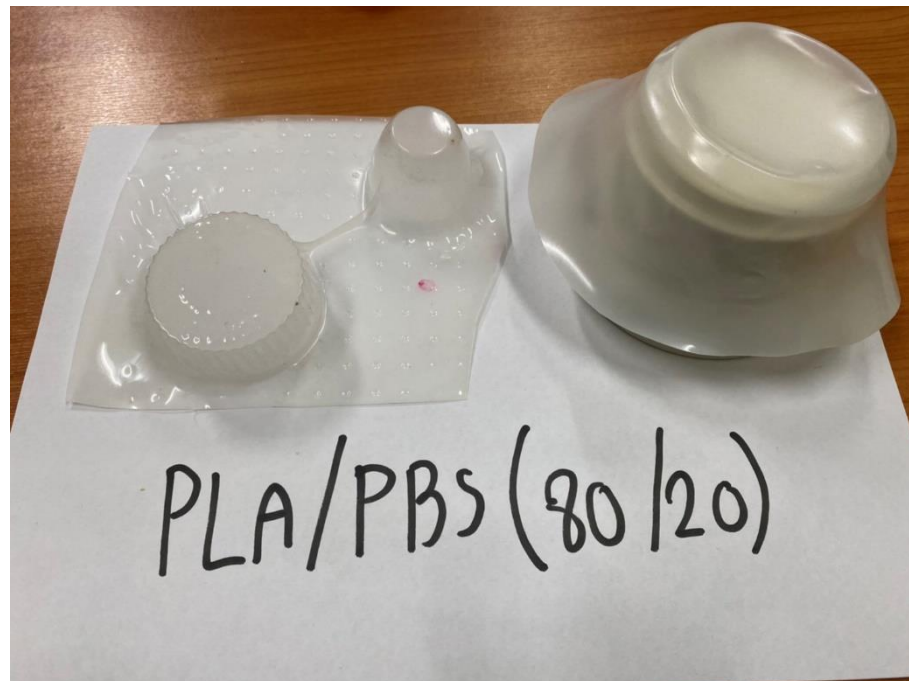


Figure 48 PLA/PBS (80/20) packaging from thermoforming

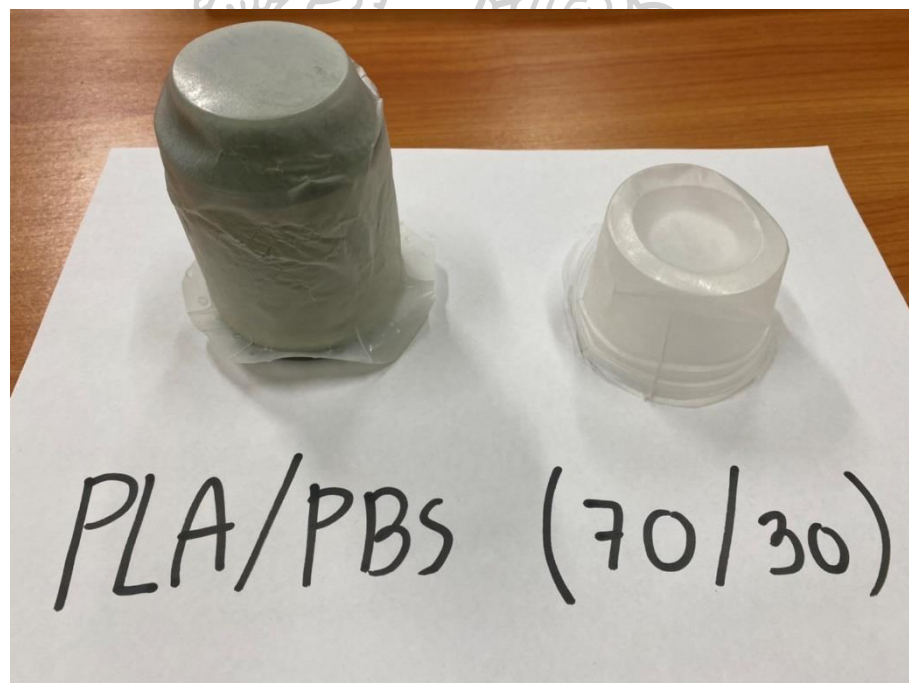


Figure 49 PLA/PBS (70/30) packaging from thermoforming

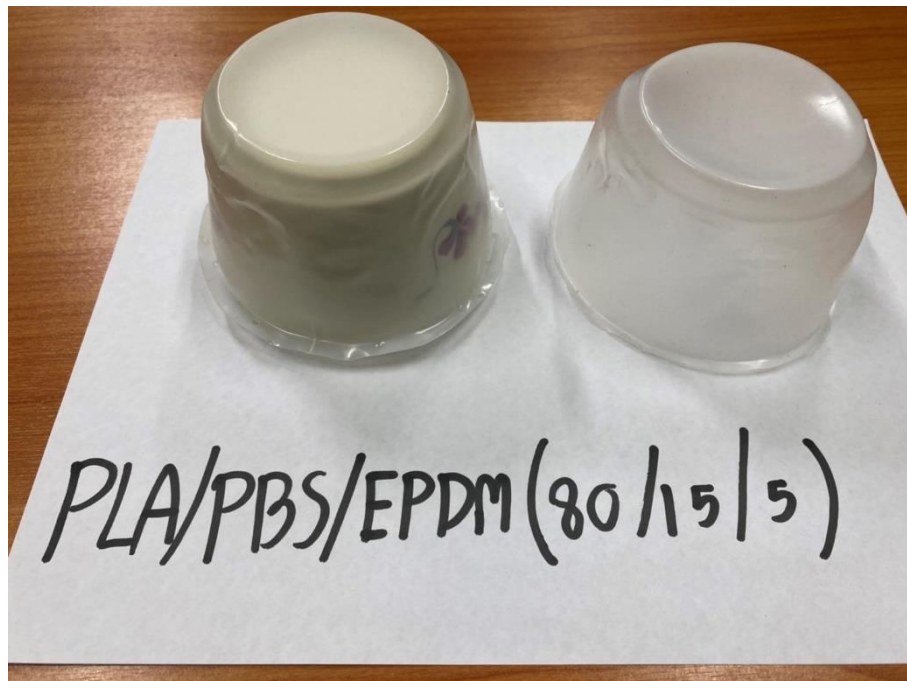


Figure 50 PLA/PBS/EPDM (80/15/5) packaging from thermoforming

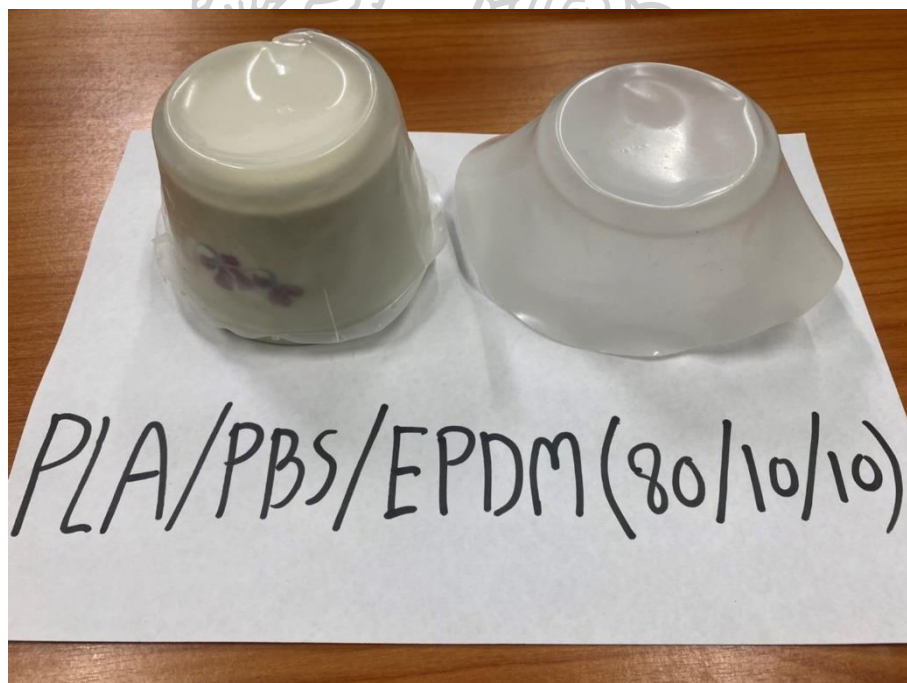


Figure 51 PLA/PBS/EPDM (80/10/10) packaging from thermoforming

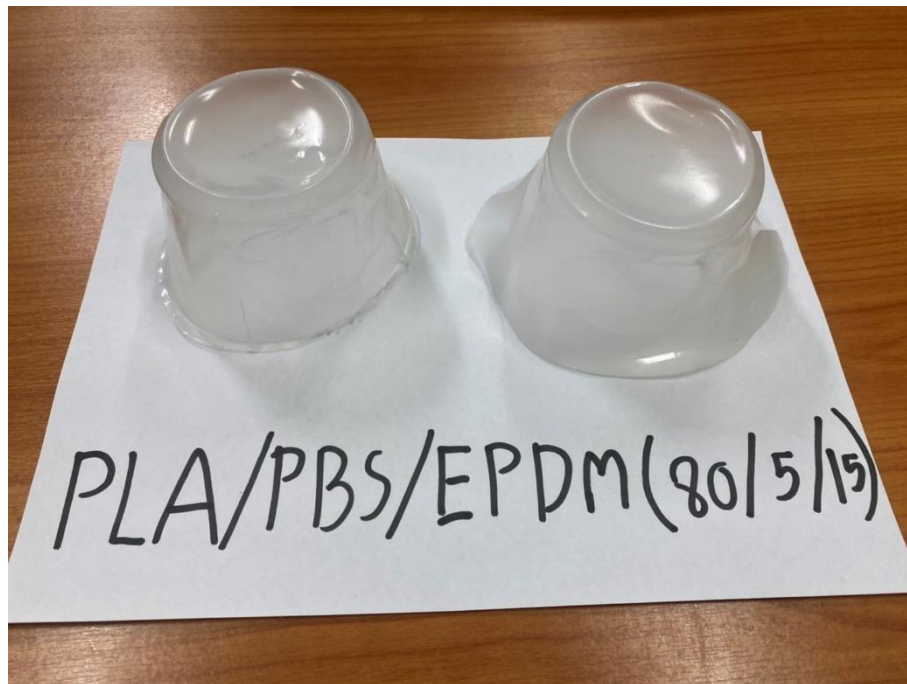
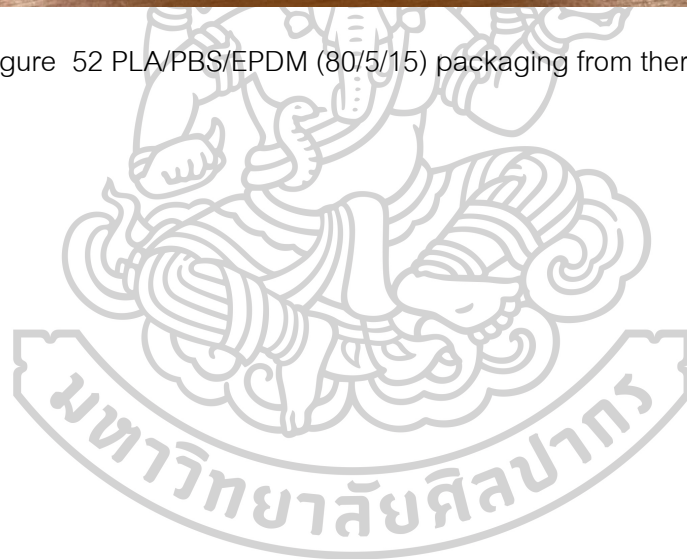


Figure 52 PLA/PBS/EPDM (80/5/15) packaging from thermoforming



CHAPTER 6

CONCLUSION

6.1 Morphological Properties

The morphology of PLA/PBS blends. The PBS phase was dispersed in PLA matrix phase and there is a circle in which the two phases were immiscible. PLA/PBS/EPDM ternary blend when increasing EPDM content affects the interoperability between the PLA and PBS phases so that they can be mixed slightly.

6.2 Mechanical Properties

The tensile strength, young's modulus, and stress at break has decreased when adding PBS content in PLA matrix at any ratio. The percent strain at break has increased when increasing PBS content. When adding EPDM the value of tensile strength, Young's modulus, and stress at break has to drop significantly.

6.3 Thermal Properties

All the PLA/PBS and PLA/PBS/EPDM blends had a lower crystallinity than pure PLA. The decomposition temperature at 5, 10 and 50% weight loss (Td5, Td10, and Td50) of pure PLA, PLA/PBS and PLA/PBS/EPDM ternary blends enhanced change slightly when compared with PLA.

6.4 Thermomechanical Properties

The storage modulus of polymer blends tended to decrease when the temperature increased. The pure PLA had higher storage modulus than PLA/PBS and PLA/PBS/EPDM ternary blends

6.5 FT-IR Analysis

Both the PLA and the PBS could be mixed to some extent due to the interaction between the carbonyl oxygen (C=O) or carbonyl group (C-O) and the oxygen hydrogen (OH) at the chain end of both PLA and PBS. Since there was no discernible change in the FTIR spectra of ternary mixes, it can be concluded that the mixtures of PLA and EPDM are incompatible with one another due to the absence of any modifications.

6.6 UV-vis analysis

The UV adsorption result, PLA/PBS blends and PLA/PBS/EPDM ternary blends can adsorb the UV light better than pure PLA.

6.7 Packaging from Thermoforming

Packaging made from PLA and PBS is brittle and thin. Especially when PLA is combined with PBS, it is not suitable for thermoforming as packaging. The packaging made from the PLA/PBS/EPDM ternary blend is stronger and thicker than packaging made from the PLA/PBS blend. However, the optimal ratios for employing PLA/PBS/EPDM packaging are PLA/PBS/EPDM (80/15/5), PLA/PBS/EPDM (80/10/10), and PLA/PBS/EPDM (80/5/15) due to the mechanical properties of these ratios being comparable to those of commercial packaging films. The precise thickness; without it, PLA/PBS/EPDM cannot be thermoformed into the package without faults.

REFERENCES

- [1] S. o. t. planet. "The Truth About Bioplastics," <https://news.climate.columbia.edu/2017/12/13/the-truth-about-bioplastics/>.
- [2] S. Farah, D. G. Anderson, and R. Langer, "Physical and mechanical properties of PLA, and their functions in widespread applications—A comprehensive review," *Advanced drug delivery reviews*, vol. 107, pp. 367-392, 2016.
- [3] J. Flynt. "Polylactic Acid (PLA): The Environment-friendly Plastic," <https://3dinsider.com/what-is-pla/>.
- [4] L.-T. Lim, R. Auras, and M. Rubino, "Processing technologies for poly (lactic acid)," *Progress in polymer science* vol. 33, no. 8, pp. 820-852, 2008.
- [5] A. Larson, K. O'Brien, and A. Anderson, "Natureworks: Green Chemistry's Contribution to Biotechnology, Innovation, Commercialization, and Strategic Positioning," 2010.
- [6] O. ECOTEXTILES. "WHAT IS THE BENEFIT OF PLA?," <https://oecotextiles.blog/2018/10/09/what-is-the-benefit-of-pla/>.
- [7] T. Casalini, F. Rossi, A. Castrovinci *et al.*, "A perspective on polylactic acid-based polymers use for nanoparticles synthesis and applications," *Frontiers in bioengineering biotechnology* pp. 259, 2019.
- [8] I. Armentano, N. Bitinis, E. Fortunati *et al.*, "Multifunctional nanostructured PLA materials for packaging and tissue engineering," *Progress in Polymer Science*, vol. 38, no. 10-11, pp. 1720-1747, 2013.
- [9] J. Muller, C. González-Martínez, and A. Chiralt, "Combination of poly (lactic) acid and starch for biodegradable food packaging," *Materials*, vol. 10, no. 8, pp. 952, 2017.
- [10] N. Jacquél, F. Freyermouth, F. Fenouillot *et al.*, "Synthesis and properties of poly (butylene succinate): Efficiency of different transesterification catalysts," *Journal of*

Polymer Science Part A: Polymer Chemistry

vol. 49, no. 24, pp. 5301-5312, 2011.

- [11] J. Xu, and B. H. Guo, "Poly (butylene succinate) and its copolymers: Research, development and industrialization," *Biotechnology journal*, vol. 5, no. 11, pp. 1149-1163, 2010.
- [12] Z. M. Rzayev, B. A. Göçmen, D. Demircan *et al.*, "EPDM Elastomer and Biothermoplastic Polyester-based Silicate-layered Multifunctional Nanocomposites Incorporated with Poly (MA-alt- α -olefin)-g-APTS-SiO₂ NPs and PP-g-MA by Reactive Extrusion Nanotechnology," *Polymer-Plastics Technology*

Engineering

vol. 56, no. 17, pp. 1839-1856, 2017.

- [13] A. M. Hasan, and M. E.-S. Abdel-Raouf, "Cellulose-based superabsorbent hydrogels," *Cellulose-Based Superabsorbent Hydrogels. Springer International Publishing*, pp. 245-267, 2019.
- [14] Geoff. "The Principle of Thermoforming," <http://www.euroextrusions.com/the-principle-of-thermoforming/>.
- [15] G. Editor. "Tensile Test or Tensile Testing," <https://guidebytips.com/tensile-test/>.
- [16] V. Shah, *Handbook of plastics testing and failure analysis*: John Wiley & Sons, 2020.
- [17] K. Akhtar, S. A. Khan, S. B. Khan *et al.*, "Scanning electron microscopy: principle and applications in nanomaterials characterization," *Handbook of materials characterization*, pp. 113-145: Springer, 2018.
- [18] E.-C. Stefanaki, "Electron microscopy: the basics," *Physics of advanced materials winter school*
- vol. 4, pp. 1-11, 2008.
- [19] A. Osahor, K. Deekonda, C.-W. Lee *et al.*, "Rapid preparation of adherent mammalian cells for basic scanning electron microscopy (SEM) analysis," *Analytical biochemistry*, vol. 534, pp. 46-48, 2017.

- [20] G. Höhne, J. McNaughton, W. Hemminger *et al.*, *Differential scanning calorimetry*: Springer Science & Business Media, 2003.
- [21] P. Gill, T. T. Moghadam, and B. Ranjbar, "Differential scanning calorimetry techniques: applications in biology and nanoscience," *Journal of biomolecular techniques: JBT*, vol. 21, no. 4, pp. 167, 2010.
- [22] N. P. Cheremisinoff, *Polymer characterization: laboratory techniques and analysis*: William Andrew, 1996.
- [23] R. Artiaga, R. Cao, S. Naya *et al.*, *Separation of overlapping processes from TGA data and verification by EGA*, 2007.
- [24] A. Gorassini, P. Calvini, and A. Baldin, "Fourier Transform Infrared Spectroscopy (FTIR) Analysis of Historic Paper Documents as a Preliminary Step for Chemometrical Analysis," 01/01, 2008.
- [25] C. Maxwell, C. Kennedy, T. Wess *et al.*, *X-Ray diffraction analysis of paper samples – Investigation into the effects of water, deacidification treatments and artificial ageing process on cellulose crystallinity*, 2008.
- [26] J. Roberts, A. Power, J. Chapman *et al.*, "The Use of UV-Vis Spectroscopy in Bioprocess and Fermentation Monitoring," *Fermentation*, vol. 4, 03/13, 2018.
- [27] T. Yokohara, K. Okamoto, and M. Yamaguchi, "Effect of the shape of dispersed particles on the thermal and mechanical properties of biomass polymer blends composed of poly (L-lactide) and poly (butylene succinate)," *Journal of applied polymer science*, vol. 117, no. 4, pp. 2226-2232, 2010.
- [28] T. Yokohara, and M. Yamaguchi, "Structure and properties for biomass-based polyester blends of PLA and PBS," *J European Polymer Journal*, vol. 44, no. 3, pp. 677-685, 2008.
- [29] N. Bitinis, R. Verdejo, P. Cassagnau *et al.*, "Structure and properties of polylactide/natural rubber blends," *Materials Chemistry* vol. 129, no. 3, pp. 823-831, 2011.
- [30] D. H. Park, M. S. Kim, J. H. Yang *et al.*, "Effects of compatibilizers and hydrolysis on the mechanical and rheological properties of polypropylene/EPDM/poly (lactic

- acid) ternary blends," *Macromolecular Research*, vol. 19, no. 2, pp. 105-112, 2011.
- [31] Y. Huang, C. Zhang, Y. Pan *et al.*, "Study on the effect of dicumyl peroxide on structure and properties of poly (lactic acid)/natural rubber blend," *Journal of Polymers the Environment* vol. 21, no. 2, pp. 375-387, 2013.
- [32] D. Bigg, "Polylactide copolymers: Effect of copolymer ratio and end capping on their properties," *Advances in Polymer Technology: Journal of the Polymer Processing Institute* vol. 24, no. 2, pp. 69-82, 2005.
- [33] M. M. F. Ferrarezi, M. de Oliveira Taipina, L. C. Escobar da Silva *et al.*, "Poly (ethylene glycol) as a compatibilizer for poly (lactic acid)/thermoplastic starch blends," *Journal of Polymers the Environment*, vol. 21, no. 1, pp. 151-159, 2013.
- [34] S. Su, R. Kopitzky, S. Tolga *et al.*, "polymers Review Polylactide (PLA) and Its Blends with Poly(butylene succinate) (PBS): A Brief Review," *Polymers*, vol. 11, pp. 1193, 07/17, 2019.
- [35] M. Mehrabi Mazidi, and M. K. Razavi Aghjeh, "Synergistic Toughening Effects of Dispersed Components in PP/PA6/EPDM Ternary Blends; Quantitative Analysis of the Fracture Toughness via the Essential Work of Fracture (EWF) Methodology," *RSC Adv.*, vol. 5, 05/21, 2015.
- [36] A. Piontek, O. Vernaes, and S. Kabasci, "Compatibilization of Poly(Lactic Acid) (PLA) and Bio-Based Ethylene-Propylene-Diene-Rubber (EPDM) via Reactive Extrusion with Different Coagents," *Polymers*, vol. 12, pp. 605, 03/06, 2020.
- [37] S. Wang, S. Pang, L. Pan *et al.*, "Compatibilization of poly(lactic acid)/ethylene-propylene-diene rubber blends by using organic montmorillonite as a compatibilizer," *Journal of Applied Polymer Science*, vol. 133, 08/01, 2016.
- [38] F. A. dos Santos, Tavares, Maria Inês Bruno "Development of biopolymer/cellulose/silica nanostructured hybrid materials and their

- characterization by NMR relaxometry," *Polymer Testing*, vol. 47, pp. 92-100, 2015.
- [39] V. G. Silverajah, N. A. Ibrahim, N. Zainuddin *et al.*, "Mechanical, thermal and morphological properties of poly (lactic acid)/epoxidized palm olein blend," *Molecules*, vol. 17, no. 10, pp. 11729-11747, 2012.
- [40] L. Chongad, A. Sharma, M. Banerjee *et al.*, "Synthesis of lead sulfide nanoparticles by chemical precipitation method." p. 012032.
- [41] K. F. El-Nemr, M. A. M. Ali, S. N. Saleh *et al.*, "Mechanical properties of gamma-irradiated styrene-butadiene rubber/acid-treated vermiculite clay/maleic anhydride nanocomposites," vol. 59, no. 2, pp. 355-364, 2019.
- [42] J.-t. Yeh, C.-H. Tsou, Y.-m. Li *et al.*, "The compatible and mechanical properties of biodegradable poly(Lactic Acid)/ethylene glycidyl methacrylate copolymer blends," *Journal of Polymer Research*, vol. 19, 02/01, 2012.
- [43] G. Craciun, E. Manaila, D. Ighigeanu *et al.*, "A Method to Improve the Characteristics of EPDM Rubber Based Eco-Composites with Electron Beam," *Polymers*, vol. 12, pp. 215, 01/15, 2020.
- [44] G. Barra, J. Crespo, B. R *et al.*, "Maleic Anhydride Grafting on EPDM: Qualitative and Quantitative Determination," *Journal of the Brazilian Chemical Society*, vol. 10, 01/01, 1999.
- [45] R. Chitta, A. Ginzburg, G. v. Doremaele *et al.*, "Separating ethylene-propylene-diene terpolymers according to the content of diene by HT-HPLC and HT 2D-LC," *Polymer*, vol. 52, pp. 5953-5960, 2011.



VITA

NAME Laoongpun Wongwad

DATE OF BIRTH 26 August 1993

PLACE OF BIRTH Phetchabun

INSTITUTIONS ATTENDED Bachelor of Engineering (Chemical Engineering)
Rangsit University

HOME ADDRESS 56/2 Moo 1 Rama 2 Rd., Khok Krabue, Amphoe Mueang
Samut Sakhon, Samut Sakhon, 74000.

